A CASE STUDY FOR CALCULATING AND REPORTING THE UNCERTAINTY BUDGET OF 1 AND 2 DIMENSIONAL COMBINED HYDRAULIC MODEL

A THESIS SUBMITTED TO
THE GRADUATE SCHOOL OF NATURAL AND APPLIED SCIENCES
OF
MIDDLE EAST TECHNICAL UNIVERSITY

BY

UĞRAŞ SİDAR GÜL

IN PARTIAL FULFILLMENT OF THE REQUIREMENTS
FOR
THE DEGREE OF MASTER OF SCIENCE
IN
CIVIL ENGINEERING

AUGUST 2019

Approval of the thesis:

A CASE STUDY FOR CALCULATING AND REPORTING THE UNCERTAINTY BUDGET OF 1 AND 2 DIMENSIONAL COMBINED HYDRAULIC MODEL

submitted by **UĞRAŞ SİDAR GÜL** in partial fulfillment of the requirements for the degree of **Master of Science in Civil Engineering Department, Middle East Technical University** by,

Prof. Dr. Halil Kalıpçılar
Dean, Graduate School of **Natural and Applied Sciences** ________________

Prof. Dr. Ahmet Türer
Head of Department, **Civil Engineering** ________________

Prof. Dr. Ayşe Burcu Altan Sakarya
Supervisor, **Civil Engineering, METU** ________________

Examining Committee Members:

Prof. Dr. Mete Köken
Civil Engineering, METU ________________

Prof. Dr. Ayşe Burcu Altan Sakarya
Civil Engineering, METU ________________

Prof. Dr. Mehmet Ali Kökpınar
Civil Engineering, TED University ________________

Dr. Elif Oğuz
Civil Engineering, METU ________________

Dr. Önder Koçyiğit
Civil Engineering, Gazi University ________________

Date: 29.08.2019

I hereby declare that all information in this document has been obtained and presented in accordance with academic rules and ethical conduct. I also declare that, as required by these rules and conduct, I have fully cited and referenced all material and results that are not original to this work.

Name, Surname: Uğraş Sidar Gül

Signature:

ABSTRACT

A CASE STUDY FOR CALCULATING AND REPORTING THE UNCERTAINTY BUDGET OF 1 AND 2 DIMENSIONAL COMBINED HYDRAULIC MODEL

Gül, Uğraş Sidar
Master of Science, Civil Engineering
Supervisor: Prof. Dr. Ayşe Burcu Altan Sakarya

August 2019, 70 pages

This study aims to suggest a framework to quantify and report the uncertainty budget of a 1 & 2 dimensional hydraulic model of five possible error sources by using ISO GUM method.

The river engineers take into account several considerations when they design the riverbeds; one of the main considerations is the flood protection aspect of the riverbed, to asses that a hydraulic model is usually prepared. However, results generated from the hydraulic models are not exempt from errors. The ISO GUM method provides guidelines and specifications to express combined uncertainties to quantify and report these errors.

The reference model -which is derived from a case study in Kemalpaşa, Artvin Turkey- lies in the center of data generation. Treating the reference model as a laboratory, by manipulating the reference model with custom VBA codes and exporting result with Python codes, an extensive set of data from 3825 model runs were generated for five error sources. The measurement in this study is the maximum water surface levels in meters.

As a result, the uncertainty budgets of 16 cross sections and 14 two-dimensional computational cells were calculated. It is foreseen that the variations in input parameters result in a maximum combined uncertainty of ± 0.454 m for cross sections and ± 0.664 m for 2-dimensional computational cells at 95% confidence level with coverage factor of 1.96 . It would be safe to say that the majority of the error is due to the variation in Manning's n coefficient.

Keywords: Uncertainty Budget, ISO GUM, Hydraulic Modelling, Uncertainty in Measurement, HEC-RAS

ÖZ

BİR ÖRNEK OLAY ÇERÇEVESİNDE İNCELENMİŞ 1 VE 2 BOYUTLU BİRLEŞTİRİLMİŞ HİDROLİK MODELİN BELİRSİZLİK BÜTÇESİNİN HESAPLANMASI VE RAPORLANMASI

Gül, Uğraş Sidar
Yüksek Lisans, İnşaat Mühendisliği
Tez Danışmanı: Prof. Dr. Ayşe Burcu Altan Sakarya

Ağustos 2019, 70 sayfa

Bu çalışma, 1 & 2 boyutlu bir hidrolik modelin, beş olası hata kaynağının belirsizlik bütçesini ISO GUM yöntemini kullanarak ölçmek ve raporlamak için bir çerçeve önermeyi amaçlamaktadır.

Nehir mühendisleri, nehir yataklarını tasarlarken bazı hususları dikkate alır; önemli hususlardan biri, nehir yatağının taşkın koruma yönüdür, bunun için genellikle bir hidrolik model hazırlanır. Ancak, hidrolik modellerden elde edilen sonuçlar hatalardan muaf değildir. ISO GUM yöntemi, bu hataların birleşik belirsizlikler olarak ölçülmesi ve raporlanması için kılavuzlar ve şartları sağlar.

Artvin Türkiye, Kemalpaşa'daki bir örnek olay incelemesinden elde edilen referans model, veri üretiminin merkezindedir. Referans modelinin bir laboratuvar olarak ele alınması, referans modelinin özel VBA kodları ile manipüle edilmesi ve sonucun Python kodları ile dışa aktarılmasıyla, beş hata kaynağı için 3825 model çalışmasından kapsamlı bir veri seti üretilmiştir. Bu çalışmada yapılan ölçüm metre cinsinden maksimum su yüzey seviyesidir.

Sonuç olarak, 16 enine kesit ve 14 iki boyutlu hesaplama hücresinin belirsizlik bütçeleri hesaplanmıştır. Girdi parametrelerindeki değişikliklerin,% 95 güven

aralığında, 1.96 kapsama faktörü ile, enine kesitler için ± 0.454 m ve 2 boyutlu hesaplama hücreleri için ± 0.664 m maksimum kombine belirsizlikle sonuçlandığı görülmüştür. Hatanın çoğunluğunun Manning's n katsayısının varyasyonundan kaynaklandığını söylemek doğru olacaktır.

Anahtar Kelimeler: Belirsizlik Bütçesi, ISO GUM, Hidrolik Modelleme, Ölçüm Belirsizliği, HEC-RAS

To My Wife and My Daughter Defne

ACKNOWLEDGEMENTS

First of all, I would like to express my sincere appreciation to my supervisor Prof. Dr. Ayşe Burcu ALTAN SAKARYA for her leadership, endless support, valuable guidance, and patience throughout this study.

Besides my supervisor, I would like to thank Mr. Nurullah ÖZBEY for his guidance and valuable friendship/mentorship in my personal and professional life.

I would also like to thank to my colleagues in Akar-Su Engineering and Consulting Co. Ltd. for supporting me during my absence to conduct this study.

I would like to thank my father and my boss Mr. Erdoğan GÜL, my mother and my colleague Mrs. Güler GÜL and my sister Ms. Berfin GÜL for their patient support and endless love.

Last but not least, I could not thank enough to my beloved wife Mrs. Jessica DANSON GÜL and my daughter Defne for supporting and believing in me during my long working hours.

TABLE OF CONTENTS

LIST OF TABLES

TABLES

LIST OF FIGURES

FIGURES

LIST OF ABBREVIATIONS

ABBREVIATIONS

1D	1 Dimensional
2D	2 Dimensional
BIPM	Bureau International des Poids et Mesures
CIMP	Comité International des Poids et Mesures
CR.	Creek
DEM	Digital Elevation Model
DS	Downstream
GUM	Guide to the expression of uncertainty in measurement
HEC	Hydraulic Engineering Center
ISO	International Organization for Standardization
MWSE	Maximum Water Surface Elevation
RAS	River Analysis System
TIN	Triangulated Irregular Network
US	Upstream
USACE	United States Army Corps of Engineers
VBA	Visual Basic for Applications
WAT	Watershed Analysis Tool
WSE	Water Surface Elevation
XS	Cross Section

CHAPTER 1

INTRODUCTION

1.1. Background

The river engineering industry has undergone an immense transformation in the past 24 years since the first version of USACE's Hydraulic Engineering Center River Analysis System (HEC-RAS) was first released in 1995. Computer technology has played a key role in this transformation by increasing computation capacity, which has made it possible for river engineers to understand complex river systems using hydraulic models. River Analysis software is now irreplaceable in the industry. The engineers using this software are essentially analyzing river behavior and trying to simulate the natural phenomena in a computer environment. Needless to say, there are many parameters that the engineer needs to obtain in the field or from a laboratory-determined range to generate results from this software. Some of these parameters are subjective to the engineer who determines it and contains an accepted range of error due to several reasons, such as the complexity of the river system, the turbulent nature of water in flood conditions or the unpredictability of the riverbed in high flows. This study aims to analyze some of the potential error sources in a hydraulic model individually and in a combined manner using the methods of the International Organization for Standardization Guide to the expression of uncertainty in measurement (ISO GUM).

At the core for the need of error measurement lays scientific experiments. The question of how well an empirical result is known and whether the results of the experiments agrees with a hypothesis or theoretical prediction is a process of scientific inquiry. To be able to answer these basic questions, the uncertainty of the measured result must be quantified and reported to indicate the degree of confidence associated with the measurement (Deardorff, 2001).

Although laboratories had the need of expressing uncertainties in their results, counting uncertainty is not the only component of uncertainty measurement. Throughout the time, it was recommended that the laboratories needs to assess the total uncertainty of each measurement. Environmental Protection Agency published a report entitled “Upgrading Environmental Radiation Data” in 1980. The report was produced by an ad hoc committee of the Health Physics Society where it was recommended that uncertainty measurements should consider every likely source of inaccuracy in the results. (EPA, 2004).

Recognizing the lack of international consensus on the expression of uncertainty in measurement, in 1977, the world’s highest authority in metrology, the Comité International des Poids et Mesures (CIPM), requested that the Bureau International des Poids et Mesures (BIPM) determine the problems of laboratories around the world in reporting the total uncertainties and make recommendations. In 1993, the first version of the International Organization for Standardization Guide for the expression of uncertainty in measurement was published (JCGM, 2008). The method that was described in this guideline is used to evaluate and report the uncertainty budget of some of the major error sources of the hydraulic model.

Uncertainty analyses of hydraulic measurements are widely practiced and popular, especially for stage-discharge measurements, which are a vital part of a hydraulic system. Researchers and water resources professionals have conducted uncertainty analysis on the field measurements and have expressed their results together with the information at a 95% confidence level. The ISO has published guidelines referred to as ISO/TR 5168, Measurement of fluid flow — Estimation of uncertainty of a flowrate measurement. However, an open channel hydraulic model does not have as many background details as field and laboratory measurements do in the field of uncertainty measurement. Oubennaceur et al (2018), published “Uncertainty Analysis of a Two-

Dimensional Hydraulic Model" where they study a Two-Dimensional hydraulic model uncertainty with respect to flow rate, Manning's coefficient and topography utilizing the point of estimate method (PEM) (Oubennaceur, Chokmani, Nastev, Tanguy, & Raymond, 2018). Chacön et al.(2014) studied Flood Risk Analysis (FRA) in Hydraulic Engineering Center's (HEC) watershed analysis tool (HEC-WAT) which allows user to perform risk analysis using Monte Carlo simulation approach. Certain parameters such as hydrological and hydraulic inputs and parameters are defined as variables which allows the user to perform uncertainty analysis. A deterministic pseudo- random number generator is used in the study which shows resemblance to this study. As a result, data are collected throughout many simulations –Monte Carlo iteration continues until the coverage within certain tolerance are met- to evaluate results such as average annual damage or annual exceedance probability.

It is a fact that a robust uncertainty study is only possible with comprehensive data. The capacity of deriving this data is accelerated by certain improvements in the industry. An increase in the computational capacity of computers has played a vital role in making it possible to run thousands of simulations within a reasonable timeframe. This is in addition to robust software that has been made available, such as HEC-RAS 5.0.6, developed and distributed free of charge by the US Army Corps of Engineers. Moreover, the increase in the knowhow capacity of the automation tools used for hydraulic models has made it easier to derive extensive data from hydraulic models. Furthermore, published books, such as "Breaking the HEC-RAS Code" by Christopher Goodell (Goodell, 2014), made it possible to run thousands of simulations through automation, which would be impractical and extremely timely to achieve manually.

Uncertainty analysis of a hydraulic model allows the decision makers to see a wider picture of the problem, as upper and lower limits are included in reported results. Expressing the results probabilistically provides more information for decision makers and becomes more common with professionals due to the complex nature of the hydraulic systems. A hydraulic model's main error sources may be defined as the input data and selected hydraulic parameters. In this study, the input data, such as the topographical data and hydrological data, were not considered as an error source while five hydraulic parameters are considered as error sources. These error sources are given below:

1- Manning's n Coefficient
2- Normal Depth(Friction Slope) as Downstream Boundary Condition
3- Drag Coefficient for Bridges
4- Weir Coefficient for Bridge Decks
5- Weir Coefficient for Lateral Structures

1.2. Motivation

Professional river engineers take into account several considerations when they design the riverbeds, one of the main considerations is the flood protection aspect of the riverbed. To determine whether the riverbed's capacity is relevant for the design flow, a hydraulic model is usually prepared. However, results generated from the hydraulic models are not exempt from errors. Knowing this, engineers add a safety of margin to their calculation to determine the final design. This study is conducted to analyze and report the magnitude of errors due to variations in selected hydraulic parameters of a hydraulic model. An extensive data was derived from hydraulic models which was later used to express combined uncertainty of result of the hydraulic model utilizing the ISO GUM method.

1.3. Approach

A combination of hydraulic modeling, coding and data analysis are applied throughout the study. A step-by-step explanation of the stages followed is provided in Figure 1.1.

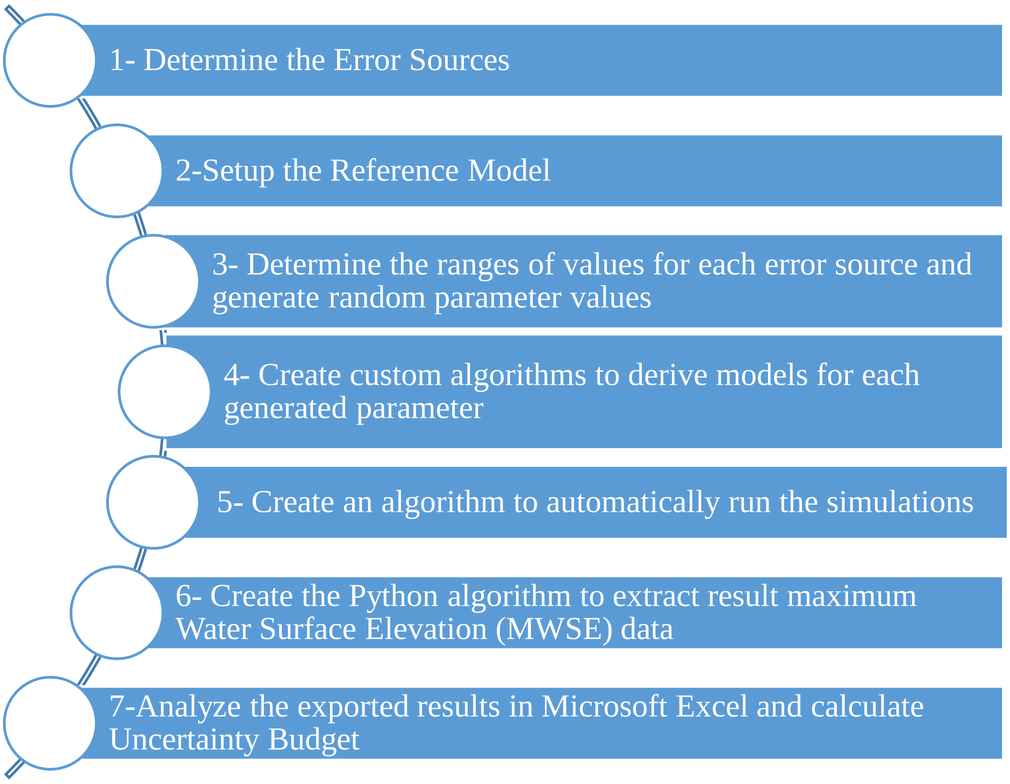

Figure 1.1: Steps defining the approach of this study

1- Determine the error sources: five parameters shown below are considered as error sources, while input data, such as topographical and hydrological data, were assumed to be true and are not included in uncertainty analysis within the scope of this study.

- Manning's n Coefficient
- Normal Depth(Friction Slope) as Downstream Boundary Condition
- Drag Coefficient for Bridges
- Weir Coefficient for Bridge Decks
- Weir Coefficient for Lateral Structures

2- Set up the reference hydraulic model: The reference hydraulic model is at the center of this study. All the generated hydraulic models are derived from the same reference model (see Figure 1.2). The reference model is a simplified version of a commercial project from the eastern Black Sea coast in Kemalpaşa, Artvin, Turkey. The results of this study do not aim to accurately show the inundation boundaries of the floods in Kemalpaşa since only a part of the project is studied and the downstream boundary condition is assumed to be Normal Depth for simplicity while in the original model the Black Sea effect was included. However, the reference hydraulic model reflects the hydraulic properties of a successfully set model, thus, it is possible to treat the hydraulic model setup as a laboratory for measuring the uncertainty of possible variations of input parameters of selected error sources.

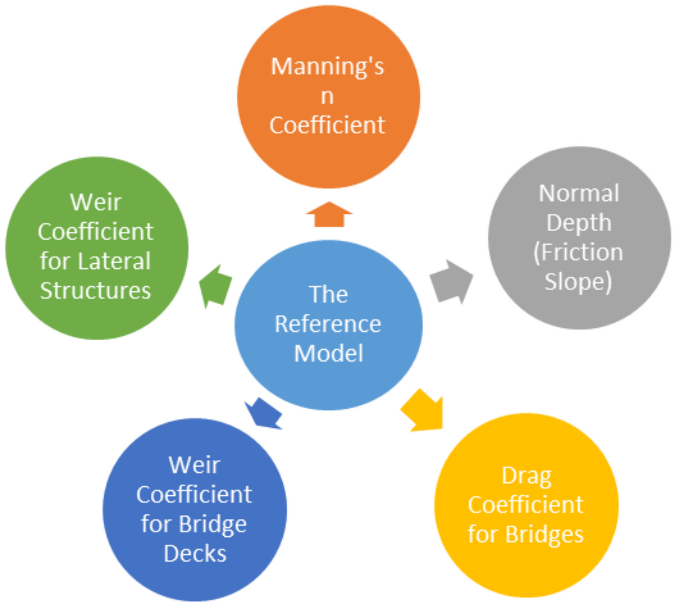

Figure 1.2: Reference model and error source parameter names.

3- Determine ranges for each error source and generate random parameters for each error source. For each error source, a likely range of values was determined. These values were determined from experience, previous research and technical manuals. The ranges for each error source and the number of generated models are provided in Table 1.1.

Table 1.1: Minimum and maximum ranges of each error sources and number of generated models

Error Source	Min	Max	# of models
Manning's n Coef.	0.020546	0.062283	870
Normal Depth (Friction Slope)	0.008198	0.013455	693
Drag Coef. for Bridges	1.092817	1.66546	778
Weir Coef. for Bridge Decks	1.251887	1.723377	792
Weir Coef. for Lateral Structures	1.04731	1.435388	692
Total			**3825**

4- Create custom algorithms to generate models for each generated parameter and generate models: The HEC-RAS file structure—extensions and file descriptions provided below—allows users to manipulate the documents using VBA on Microsoft Excel. Utilizing this method, five different VBA codes are created to automatically generate model input files for each error sources. Each code created a new model based on the reference model by changing targeted parameters with randomly generated parameters while remaining properties of the model are untouched.

Goodell (2013) states the HEC-RAS input files (for unsteady flow) as such:

.prj:The Project file. Contains current plan files, units and project description.

.g*:The Geometry file. Cross-sectional data, hydraulic structures and modeling approach data are stored here.

.p*:The Plan file. Contains a list of the associated input files and all simulation options.

.u*:The flow file extension. This is where hydrographs and initial conditions as well as any user-defined flow options are stored.

5- Create algorithm that automatically runs the simulations: A total of 3,825 models are generated with the custom codes for each error source. To run the models, a separate VBA code was adopted from Goodell (2014)'s book and all the models were run by utilizing this code; without it, it would not be possible to finish all the simulation runs within a reasonable timeframe.
6- Create the Python algorithm to export results of Max WSE (Water Surface Elevation) data: HEC-RAS 5.0.6 creates a set of different output files after the simulations are completed successfully. Several approaches may be taken to export desired outputs from the model of 1D results of cross sectional data. However, Python coding stands out when the output data of 2D cells are interested in addition to 1D cross sectional data. Considering the fact that there are 3,825 models, 684 cross sections and 7,139 2D cells, obtaining output data is possible by extracting data from *.hdf files, where all results data are stored to csv files by Python libraries such as *numpy*, *h5py* and *os* that allow users to extract data and manipulate *.hdf files.
7- Analyze the exported results in Microsoft Excel and calculate Uncertainty Budget: The extracted data from *.hdf files are imported into a Microsoft Excel spreadsheet format where statistical properties of each 1D cross section and 2D cells are analyzed in order to prepare the uncertainty budgets.

1.4. Thesis Organization

This document is prepared in 5 consecutive chapters. The chapters are aligned in a way that the reader firstly understands the background, approach and motivation, then understands the theory behind the study and finally the reader is provided with the results of the study. The results are accompanied with discussion and foreseen future works to improve this study. The brief summary of related chapters are provided below.

Chapter 1 - Introduction: The introduction chapter aims to provide a background of the thesis topic while explaining the motivation, the approach and method of the study.

Chapter 2 - Hydraulic Model: This chapters provides a brief information of what hydraulic models are and which modeling approaches are taken within the study.

Chapter 3 - Uncertainty Budget Development Using ISO GUM: Within this chapter, a brief information about ISO GUM is provided along with a step by step explanation of the approach taken in the study.

Chapter 4 - Results and Discussion: The results of combined uncertainty budgets of selected cross sections (XSs) and 2D computational cells are provided, the results are discussed and summarized.

Chapter 5 - Summary and Conclusion: In this chapter, the whole study is summarized and whether the goals at the beginning of the study is fulfilled or not is discussed. The foreseen future studies one may conduct on this topic are stated.

CHAPTER 2

HYDRAULIC MODEL

2.1. Hydraulic Model

The U.S. Army Corps of Engineers River Engineering Analysis System (HEC-RAS) is a software that allows the user to perform one–dimensional steady flow hydraulics, one and two dimensional unsteady flow river hydraulic calculations; quasi unsteady and full unsteady flow sediment transport mobile bed modeling, water temperature analysis, and generalized water quality modeling (Brunner, 2016b). The first version of HEC-RAS was released in 1995, from that day to today, the development team has increased the capabilities of the software. The 2D hydraulic calculation capabilities were added to the software beginning with version 5.0 in 2015, and the software has been continuously developed through the latest version 5.0.7.

River analysis software are where engineers try to simulate the river behaviors in a computer environment. The software such as HEC-RAS are equipped with many different tools for engineers to succeed in their works. Hydraulic models are extremely useful tools to assess and study on small or large river systems. With the expanding capabilities of mapping and computing as well as GIS extensions, it is an irreplaceable tool for engineering practices. A successfully set hydraulic model reveals the current state of a river system with an extensive set of hydraulic parameters which allow engineers to decide when and where to take action. Also, it is used for designing new channels, riverbeds and floodplains with considerable complexity, which without hydraulic simulation software would be very time consuming and error prone.

One-Dimensional (Unsteady) Hydraulic Modeling:

HEC-RAS allows user to conduct one-dimensional unsteady river simulations to estimate water surface profile along with hydraulic parameters of the river XS for each time step. In one-dimensional flow simulations the flow is assumed to be moving only x-direction while the movements in y- and z- directions are neglected.

The physical laws that govern the flow of water in a stream are: the principle of conservation of mass (continuity), and principle of conservation of momentum. Both equations are expressed mathematically in the form of partial differential equations. The conservation of mass for a control volume indicates the net rate of flow into the volume being equal to the rate of change in storage inside the volume. The momentum equation indicates that the net rate of momentum entering the volume (momentum flux) plus the sum of all external forces acting on the volume be equal to the rate of accumulation of momentum. This is a vector equation applied in x- direction. (Brunner, 2016a)

Two-Dimensional Hydraulic Modeling:

The fundamental concept of a 2D model is that the flow area is divided into a grid (computational cells) where each cell is treated as a control volume. HEC-RAS offers two different equations for 2D modelling, full 2D Saint Venant equations and 2D Diffusion Wave equations. The 2D flow solver uses an Implicit Finite Volume algorithm which allows for large computational time steps than explicit method. (Brunner, Piper, Jensen, & Chacön, 2015) The hydraulic and topographical properties of each cell is developed from the topographical data provided in the form of Digital Elevation Model. The flow is calculated in x and y direction using Saint Venant equations, which accounts for internal and external forces on the fluid, specifically hydrostatic pressure, turbulence and friction (Chacön, 2015).

Within HEC-RAS 2D modelling approach, “high resolution subgrid model” is applied (Casulli, 2008). Using this method, unlike the many other hydraulic models on the market, computational cells do not have to have a certain shape or computational cells has to have a single elevation, instead, each computational cell and cell face is based on the details of the underlying terrain. The term “subgrid” means it uses the detailed

DEM (subgrid) (see Figure 2.1) to develop the geometrical and hydraulic property tables that represent the cells and cell faces.

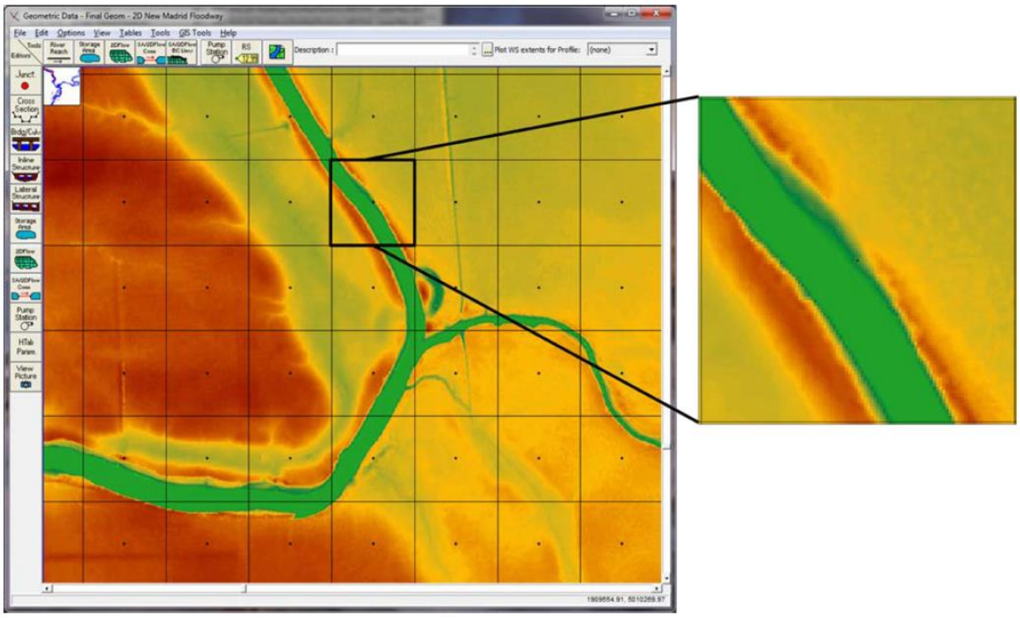

Figure 2.1: Details of underlying cell terrain data (Brunner, 2016c).

Brunner states the procedure of calculating the properties of computational cells utilizing subgrid model in HEC-RAS 5.0 as follows:

> The 2D mesh pre-processor computes a detailed elevation-volume relationship for each cell. Each cell face of a computational cell is preprocessed into a detailed hydraulic property table (elevation versus wetted perimeter, area, roughness, etc.) Following this approach, the user is able to use larger grid cell sizes than what would be possible with a model that does not preprocess the cells and cell face using the underlying terrain. (Brunner, 2016c, p3-29)

The examples of properties computational cells are provided in Figure 2.2 and Figure 2.3.

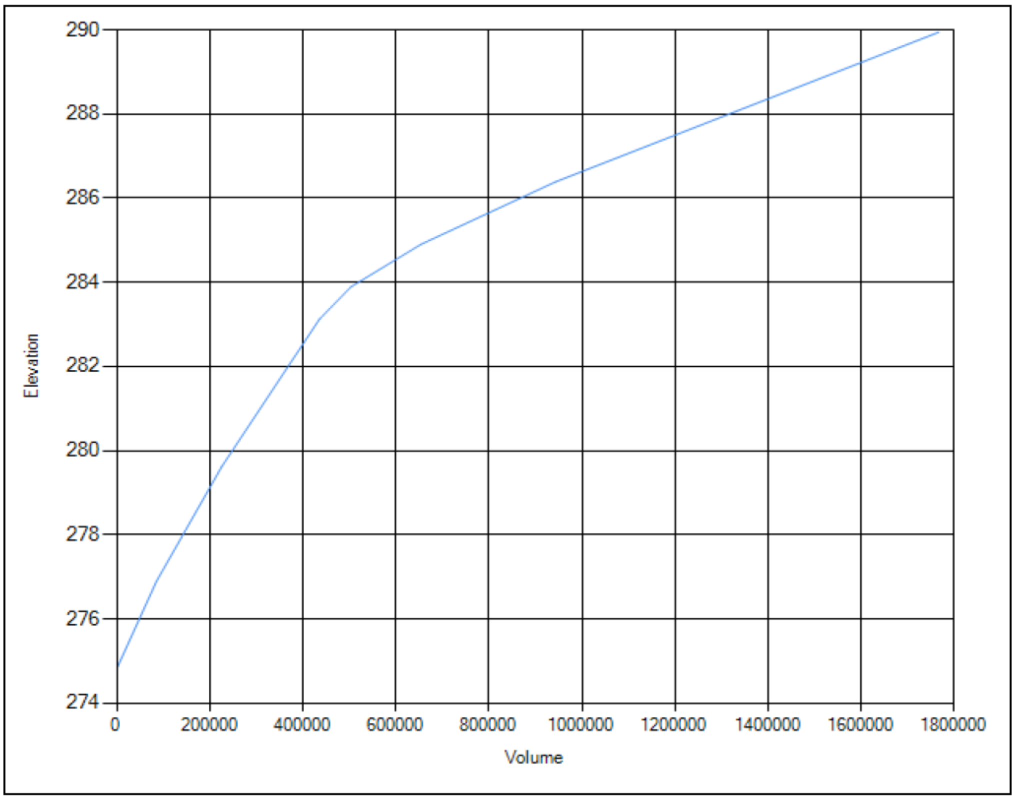

Figure 2.2: Elevation - Volume relationship for a 2D cell (Brunner, 2016c).

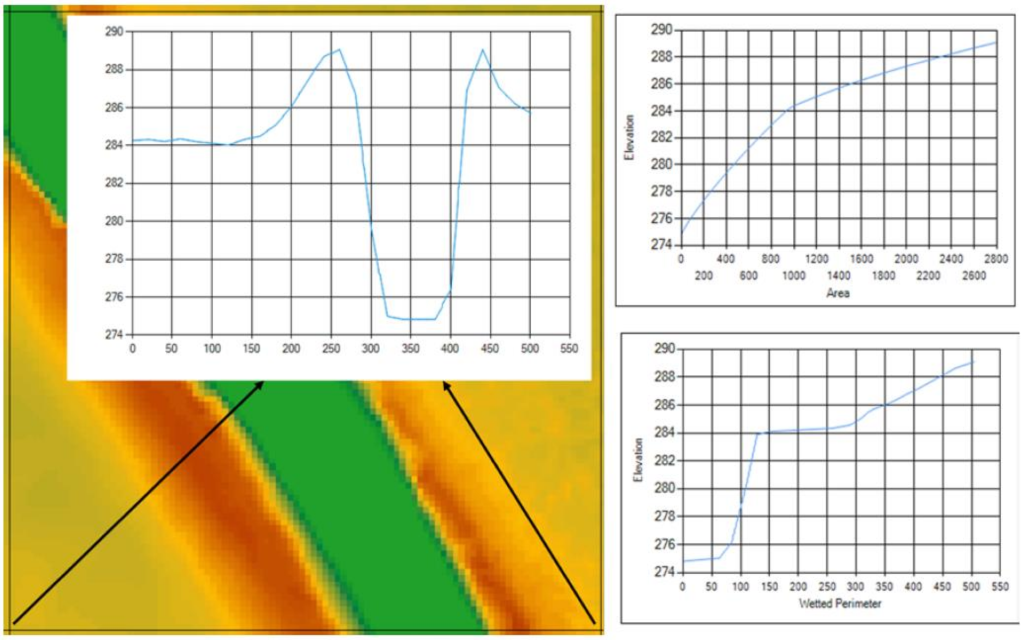

Figure 2.3: Example of how cell faces are processed into detailed cross sections and hydraulic tables (Brunner, 2016c).

One Dimensional & Two-Dimensional Combined Hydraulic Modeling:

The one-dimensional hydraulic models provide a robust solution to estimate the flow hydraulics in riverbed, however, once the water level raises above the bank lines, 1-D calculations in the floodplains, especially in urban areas, are far from being accurate. Therefore, 1D and 2D combined hydraulic models are an efficient way of assessing the likely behavior of the floods in the floodplain. The ability to perform combined 1D and 2D modelling allows user to work on large rivers systems with reduced instability and higher level of hydrodynamic fidelity (Brunner, Piper, Jensen, & Chacön, 2015). The 1D part (riverbed) of the hydraulic model is easily linked to the 2D part (floodplain) using lateral structures. The lateral weir coefficient of the lateral structure is specified when linking 1D and 2D models.

2.2. Generated Hydraulic Models

Having considered five error sources (five parameters) for this study, the generated models are based on the reference model being changed for each targeted parameter by keeping the remaining four parameters (as well as the rest of the model) untouched. For instance, to generate models to analyze the uncertainty of the Manning's n coefficient on resulting MWSE, the custom VBA code is run. The code changes target parameters (in which case the Manning's n) for each XS, while the rest of the model remains unchanged. As a result, a new model is generated with desired Manning's n values for each cross section. This way, it is possible to study the weight of the Manning's n parameter change on the MWSE as a result of 870 consecutive model runs (see Table 1.1).

2.2.1. Random Number Generation

The Box–Muller transform, a pseudo-random number sampling method, is deployed to generate normally distributed random numbers within the given standard deviations of the model inputs. Thomas, Luk, Leong, & Villasenor (2007) define the Box-Muller transformation in their studies as follows:

The Box-Muller transform is one of the earliest exact transformation methods. It produces a pair of Gaussian random numbers from a pair of uniform numbers. It utilizes the fact that the 2D distribution of two independent zero-mean Gaussian random numbers is radially symmetric if both component Gaussians have the same variance. This can be easily seen by simply multiplying the two 1D distributions $e^{-x^2}e^{-y^2} = e^{-(x^2+y^2)} = e^{-r^2}$. The Box-Muller algorithm can be understood as a method in which the output Gaussian numbers represent coordinates on the two-dimensional plane. The magnitude of the corresponding vector is obtained by transforming a uniform random number; a random phase is then generated by scaling a second uniform random number by 2π. Projections onto the coordinate axes are then performed to give the Gaussian numbers (see Figure 2.4) (Thomas, Luk, Leong, & Villasenor, 2007, p.11:5).

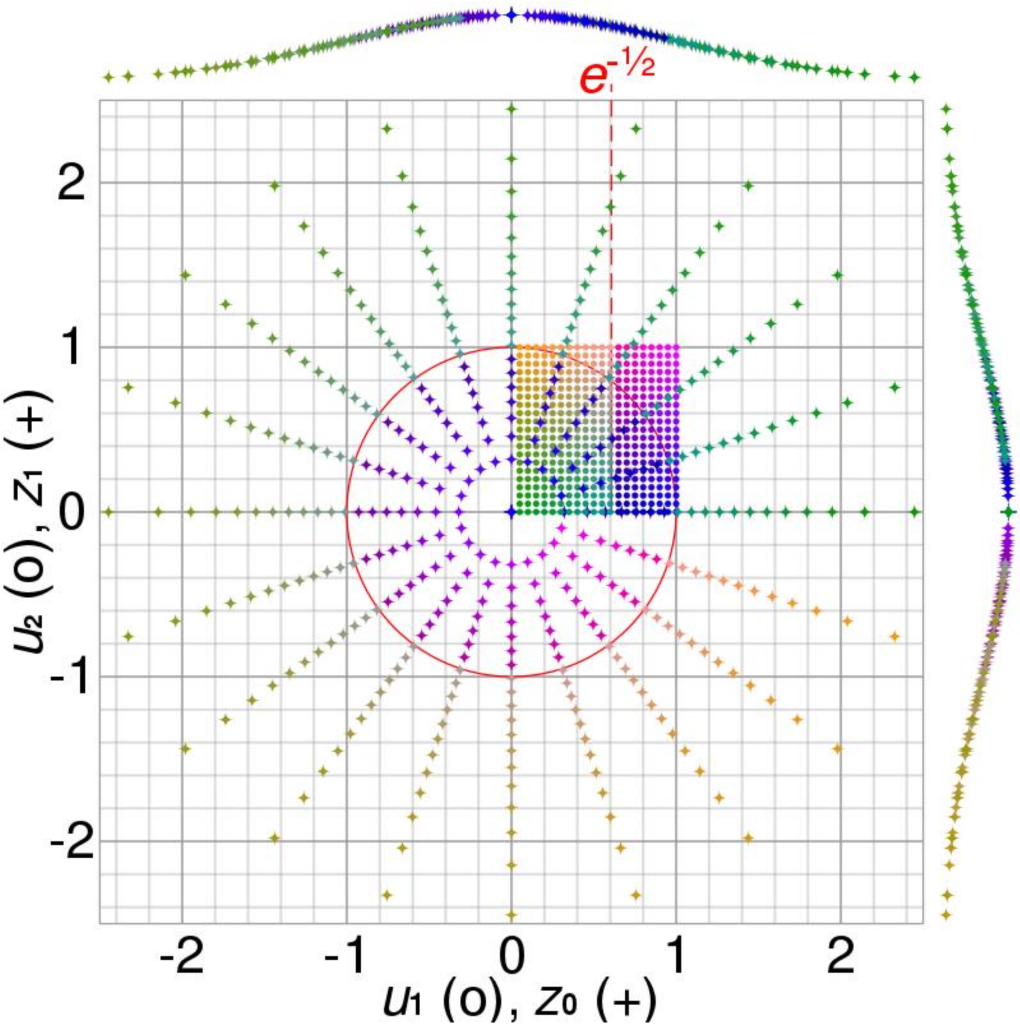

Figure 2.4: Visualization of the Box–Muller transform (Wikipedia, 2019).

The code for the Box Muller transformation random number generator is adopted from Goodell's book, "Breaking the HEC-RAS code" (Goodell, 2014).

2.2.2. Error Sources and Generated Parameters for Each Error Source

Although the hydraulic models follow a deterministic approach to calculate the MWSE and other hydraulic properties, there are many error sources in the process of setting up the model that end up as cumulative errors in the results of the model. A hydraulic model's main error sources may be defined as the input data and selected hydraulic parameters. In this study, the input data, such as the topographical data and hydrological data, were not considered as an error source while five hydraulic parameters are considered as error sources. Although there is a general consensus between professionals regarding which error sources has a bigger impacts on simulation results, it is not always possible to determine the ranges of the error sources according to a scientific measurement, therefore while some of the error ranges of below mentioned parameters are retrieved from provided sources; some of the ranges are based on experience based assumptions. These error sources are given below and detailed explanations are provided in the following chapters.

1- Manning’s n Coefficient
2- Normal Depth(Friction Slope) as Downstream Boundary Condition
3- Drag Coefficient for Bridges
4- Weir Coefficient for Bridge Decks
5- Weir Coefficient for Lateral Structures

CHAPTER 3

UNCERTAINTY BUDGET DEVELOPMENT USING ISO GUM METHOD

3.1. Uncertainty Budget Development

Every measurement is wrong. The difference between a measured value and the 'true' value of the measurand is always non-zero. In other words, no measurement or quantity that is measured (generated) from a laboratory, field or software is exempt from error. The errors may be small but also may not be (Bentley, 2005). The error of the measurements have a resulting effect on the calculations that they are based on. To understand and consider the extend of these errors, uncertainty budget calculations and sensitivity analysis plays a vital role. Having accepted this idea by scientific authorities, the need to calculate and report the errors arose. The uncertainty of the measurement and eventually uncertainty budgets are tools used to express a result with its acknowledged and calculated errors.

The uncertainty budgets may be prepared to state calibration documentation for testing the data in hand with respect to the determined uncertainty limits or for determining a tolerance level for resulting data. While analyzing the results, two numbers are needed in order to quantify an uncertainty. One is the width of the margin, or interval. The other is a confidence level, which states how sure it is that the 'true value' is within that margin (Bell, 1999). The effort for this study is to calculate an interval (combined uncertainty) for a tolerance level; throughout the world, the confidence level is adopted to be 95% for engineering studies. So, when results are indicated, engineers assume that they are 95% confident that the 'true' value is within the stated limits.

The error of resulting measurements or generated results (for this study) comes from a variety of sources. The measured instrument, the item being measured, the input data, the measurement process, calibration source, the person who operates the device or the software are all examples of error sources. This study analyzes the error sources of the modeling process, which is five input parameters entered during the process of setting up the hydraulic model.

The seven main steps that Bell (1999) provided in his study for evaluating the overall uncertainty of a measurement are provided below:

1- Decide what you need to find out from your measurements. Decide what actual measurements and calculations are needed to produce the final result.
2- Carry out the measurements needed.
3- Estimate the uncertainty of each input quantity that feeds into the final result. Express all uncertainties in similar terms.
4- Decide whether the errors of the input quantities are independent of each other. If you think not, then some extra calculations or information are needed.
5- Calculate the result of your measurement.
6- Find the combined standard uncertainty from all the individual aspects.
7- Express the uncertainty in terms of a coverage factor, together with a size of the uncertainty interval, and state a level of confidence.

Each abovementioned step is followed through in this study. The reference hydraulic model was set to be able to analyze and generate further data; in other words, the laboratory environment for this study was set with the reference hydraulic model. The MWSE of each result was analyzed for uncertainty measurement.

3.2. ISO GUM

Bentley (2005) explains the GUM as follows:

> The ISO 'Guide to the Expression of Uncertainty in Measurement', or GUM, deals with nomenclature and methods of evaluating, combining and reporting uncertainties. The GUM discusses the mathematical and statistical principals involved in the analysis of errors and defines many of the terms that have been

> used in the past to express uncertainty. In essence, the GUM summarizes available wisdom and presents a consensus on how the uncertainty in measurement should be dealt with. (Bentley, 2005, p.1)

The ISO GUM follows a certain set of procedures while preparing the uncertainty budget. These procedures are prepared for any kind of measurement and answer a wide variety of needs. This study utilizes only a part of the procedures, thus, only the details of the adapted procedures will be discussed.

Before starting the analysis of measurement uncertainty, it is essential to assess the quality and quantity of the resulting data. According to this information, the guide directs the user to adapt certain procedures. The ISO GUM provides information for four different kinds of error distributions, namely, the Gaussian (Normal) distribution, the rectangular distribution, the triangular distribution and U-distribution. In this study, an extensive dataset resulting from a total of 3,825 simulations are analyzed; therefore the majority of the resulting data fits the Gaussian (Normal) distribution. The details of Gaussian distribution and analysis of resulting data are provided in further subchapters.

3.2.1. Concepts, terminologies and symbols used in the calculations of ISO GUM

It is necessary to understand concepts, terminologies and symbols that are used in the study, because the extent of the GUM easily confuses users since the document is prepared to answer a wide variety of problems, whereas in this study a very favorable dataset is obtained for such a study. Therefore, only the parts of the GUM that were included in this study will be discussed. While the symbols might differ from source to source, the information in the further subchapters and descriptions stated here are based on Bentley (2005)'s study of 'Uncertainty in Measurement: The ISO Guide, Monograph 1'.

The Gaussian distribution:

One of the most important distributions to analyze error measurements is the Gaussian (Normal) distribution. The probability of finding an error in any given region, between any two values, is equal to the area under the curve between these values (Bentley, 2005). The ideal shape of the distribution is shown in Figure 3.1.

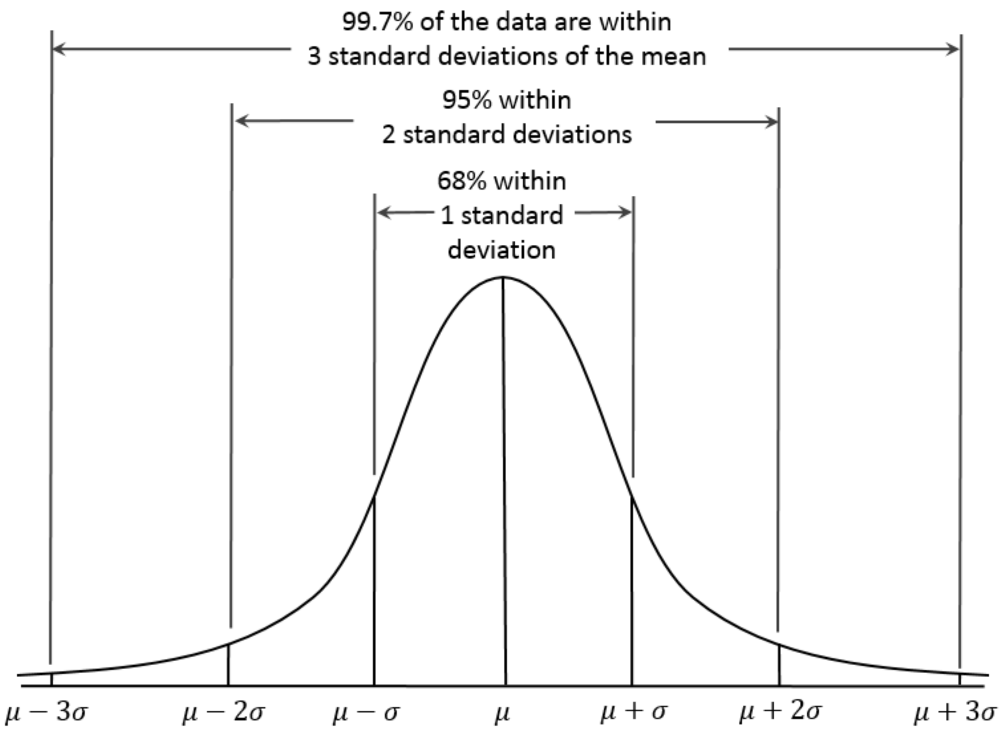

Figure 3.1: The ideal shape of a Gaussian distribution and its relation to mean and standard deviation.

It is expected that most readings occur centrally, around the average of all the readings (the mean). There were as much data above the means as there were below it; and, the further away from the mean, the fewer the readings. The curve that represents the data is known as a Gaussian curve. The Gaussian function best describes most causes of fluctuations in the data.

Raw Error Estimates:

Type A evaluation: method of evaluation of uncertainty by statistical analysis of series of observations.

Type B: Error method of evaluation of uncertainty by means other than the statistical analysis of series of observations (JCGM, 2008) In other words, Type B estimates are from any other information, such as past experience, calibration results, etc.

Within the context of this study, the error estimates are Type A components.

Standard uncertainty

The calculation procedure recommended in the ISO GUM requires values of standard deviation for each error source. Each is referred to as a 'standard uncertainty'. For the input quantity x_i, a standard uncertainty is given the symbol $u(x_i)$.

The standard uncertainties of $u(x_i)$ are calculated from the aggregated results of generated hydraulic models.

The symbol U_i

U_i represents the expanded error of a measurement represented by the equation $u(x_i)= U_i /k$.

Coverage factor *k*

Obtaining the standard deviation for an error distribution generally requires a reduction factor, depending on the type of distribution and how the width of the distribution is initially expressed and estimated. The coverage factor k is an 'expanding' factor that converts the combined standard uncertainty into expanded uncertainty U. The combined standard uncertainty is a property of a Gaussian distribution and the accepted practice is to evaluate k at 95% probability. As a result, $k \geq 1.96$, from Student's t_p at p =95%.

Sensitivity coefficient c_i

Raw uncertainty estimates relate to the input quantities—not to the measurand— and the parameter being determined from the measurement from the model. Therefore, what is required is the conversion of the raw data into their equivalents as components of uncertainty in the measurand. This process is done using sensitivity coefficient.

However, some components of uncertainty will not need a sensitivity coefficient determined, because they relate directly to the measurand (Bentley, 2005). In this case, the sensitivity coefficient, c_i, is equal to 1. In this study, all error sources are directly related to the measurand and, therefore, the sensitivity coefficient c_i is equal to 1.

Degree of freedom v_i and effective degree of freedom v_{eff}

For each source of error, the formation of an estimate of its standard deviation is needed. And, the estimate u (the standard uncertainty) is often derived from the larger quantity U_i. However, not all estimates can be treated equally since some are accurate representations of the 'true' standard deviations and some are rather poor. Some other way of having the quality of the estimates reflected in the final outcome of the calculations and the expanded uncertainty is necessary.

To do this, it is essential to measure how well each standard uncertainty has been estimated – what is the quality or reliability of each u_i. This measure is the number of degrees of freedom and is given the symbol v_i.

In ISO processes, all components of uncertainty are combined to form the 'combined standard uncertainty' u_c and its number of degrees of freedom is calculated from all the v_i's and given the symbol v_{eff}.

For Type A estimates, the number of degrees of freedom v_i is simply n-1.

3.2.2. Methodology for constructing the Uncertainty Budget

The methodology to calculate uncertainty budgets is listed in Bentley (2005)'s study, and it is as follows:

Step 1: Model the measurement

When a measurement result is expressed with its uncertainty, it normally takes the form:

$$T = T_m \pm U \quad (1)$$

where T is the 'true' value of the parameter being measured, T_m is the measured value and $\pm U$ is the uncertainty in T_m.

Step 2: List all error sources

Five error sources of model input parameters are considered within this study, which are Manning's n coefficient, normal depth of downstream boundary condition, lateral weir coefficient, bridge drag coefficient and bridge weir coefficient.

Step 3: Characterize all error components

Three values are needed for each error: U_i, k_i and v_i. The effect of each of the N errors must be evaluated/estimated as $\pm U_i$ from the raw data and a reduction factor (k_i) chosen to allow its conversion to a standard deviation.

The k_i values for samples more than 120 for 95% confidence level is assigned in Student's t distribution as 1.96.

v_i is simply n-1 for each error source dataset.

Step 4: Get components of standard uncertainty for the measurand

The standard uncertainty $u(x_i)$ is retrieved from each raw estimate U_i as U_i/k_i. This value then needs to be converted into a standard uncertainty for the measurand using the sensitivity coefficient c_i for that input quantity that U_i directly affects.

Corresponding uncertainty in measurand = $|c_i|u(x_i)$

Step 5: The combined standard uncertainty

The formula for combined uncertainty u_c^2:

$$u_c^2 = \sum |c_i.u(x_i)|^2 \tag{2}$$

$$u_c = \sqrt{\sum_{i=1}^{N} |c_i.u(x_i)|^2}. \tag{3}$$

Step 6: The expended uncertainty

$$U = k\, u_c \tag{4}$$

For value of *k*, the v_{eff} is needed.

$$v_{eff} = \frac{u_c^4}{\sum |c_i.u(x_i)|^4 / v_i} \tag{5}$$

$$k = 1.96 + \frac{2.5}{v_{eff}} + \frac{2.3}{{v_{eff}}^2} + \frac{2.2}{{v_{eff}}^3} + \frac{3.7}{{v_{eff}}^4} \tag{6}$$

Step 7: State the results

The ‘result’ of a measurement should not be considered as just the derivative value of the measurand. For it to be of practical value, it should include a statement of uncertainty, which in turn requires values of coverage probability and coverage factor.

A number of options for expressing measurement results is given in the ISO GUM. If the ± symbol is used, the ISO GUM suggests that the results:

- be given in the form: $Y=Y_m \pm U$, with the units for both Y_m and U indicated
- both Y_m, the calculated/measured value of measurand, and U should be rounded to the same level
- the level of confidence be stated (95%) and

the coverage factor *k* is given.

CHAPTER 4

RESULTS AND DISCUSSION

4.1. The Reference Model

The reference model is a simplified version of a commercial project in the eastern Black Sea coast in Kemalpaşa, Artvin, Turkey. The results of this study do not aim to accurately show the inundation boundaries of the flood extend in Kemalpaşa since only a part of the project is considered and downstream boundary is assumed to be Normal Depth for simplicity while in the original model the Black Sea effect was included. However, the reference hydraulic model reflects the hydraulic properties of a successfully set model, thus, it is possible to treat the hydraulic model setup as a laboratory for measuring the uncertainty of possible variations of input parameters of selected error sources.

4.1.1. Study Area

The study takes place in Kemalpaşa town in Artvin province by the east coast of the Black Sea adjacent to the Turkish - Georgian boarder. Two of the creeks, Köprücü and Çam creeks, are modeled within the study. The Köprücü and Çam creeks merge and then discharges to the Black Sea (see Figure 4.1). Unlike the typical topography of the eastern Black Sea in Turkey, the slope of the hills is formed with milder slopes; and, the average slope of the Köprücü Creek in the study area is 0.02 while the average slope of the Çam Creek is 0.01. The majority of the settlements take place by the downstream of the creeks.

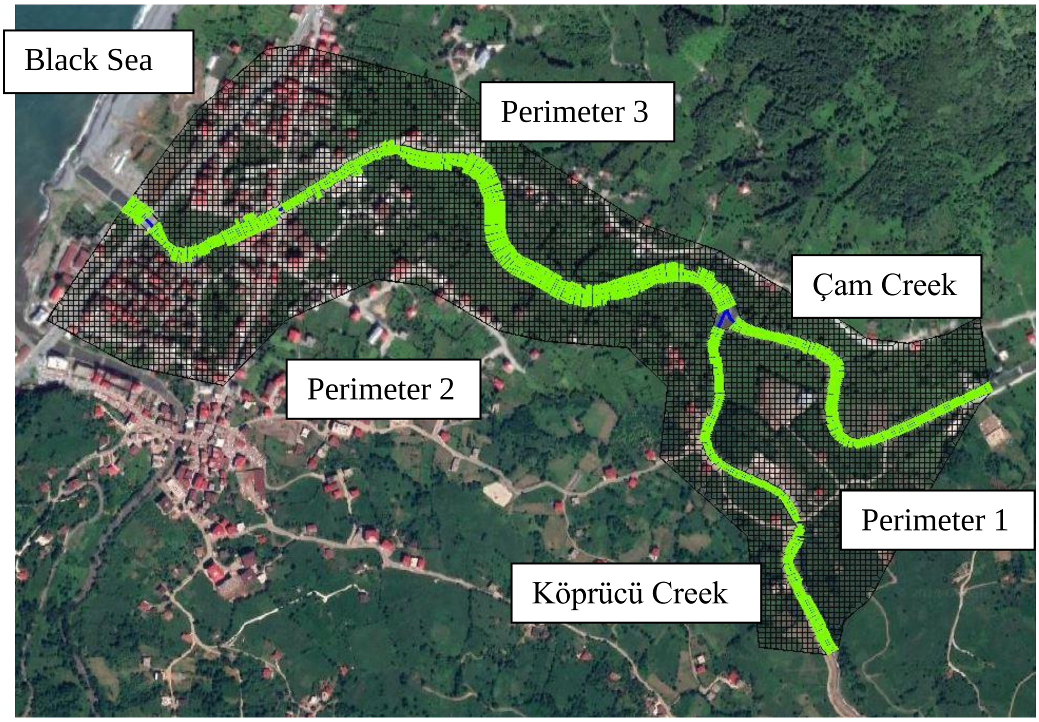

Figure 4.1: Hydraulic model extends of 2D mesh, XSs and river network.

4.1.2. Topographical Survey Data

The Triangulated Irregular Network (TIN) and the Digital Elevation Model (see Figure 4.2 and Figure 4.3) are generated from the data collected by an instrument whose accuracy is Real-Time Kinematic (RTK) positioning 'H 1cm+1ppm, V 2cm+1ppm' and PP 'H '0.25cm+1ppm, V 0.5cm+1ppm' with a confidence level of 99.9%. The digital elevation models (DEM) generated from a ground-based differential GPS (DGPS) survey contained more than 41,263 points within the 2.33 km^2. (SATLAB Geosolutions, 2014)

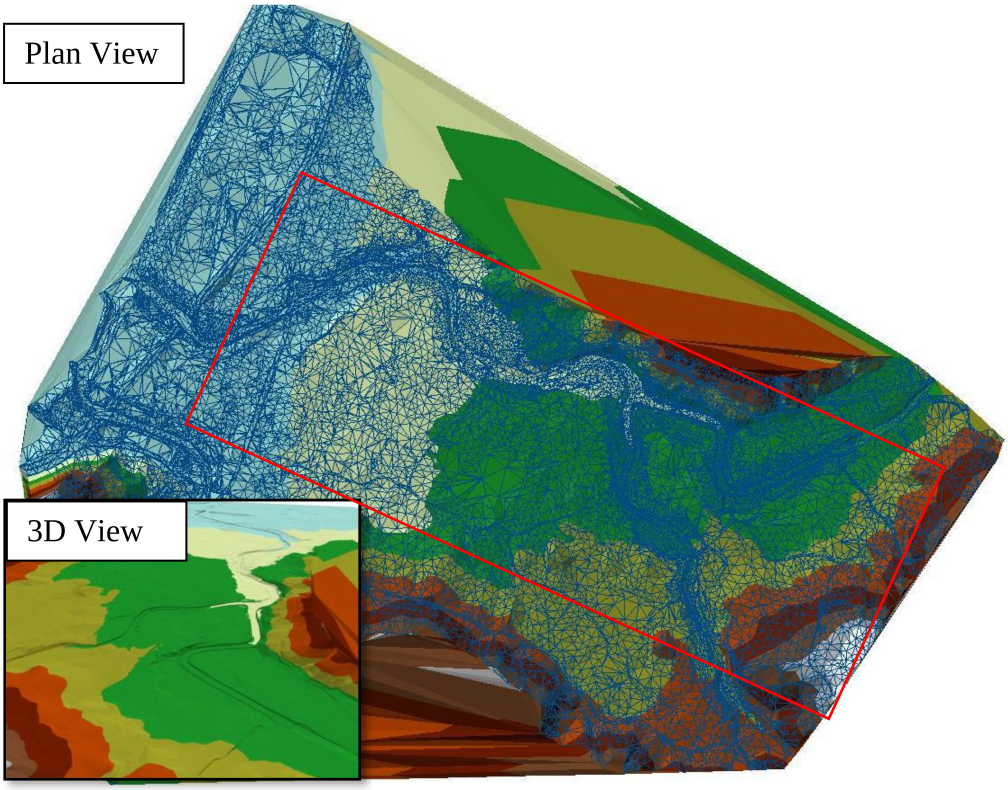

Figure 4.2: The TIN (Triangulated Irregular Network) model created from topographical surveys, the 3D view of TIN model, extends shown by the red frame.

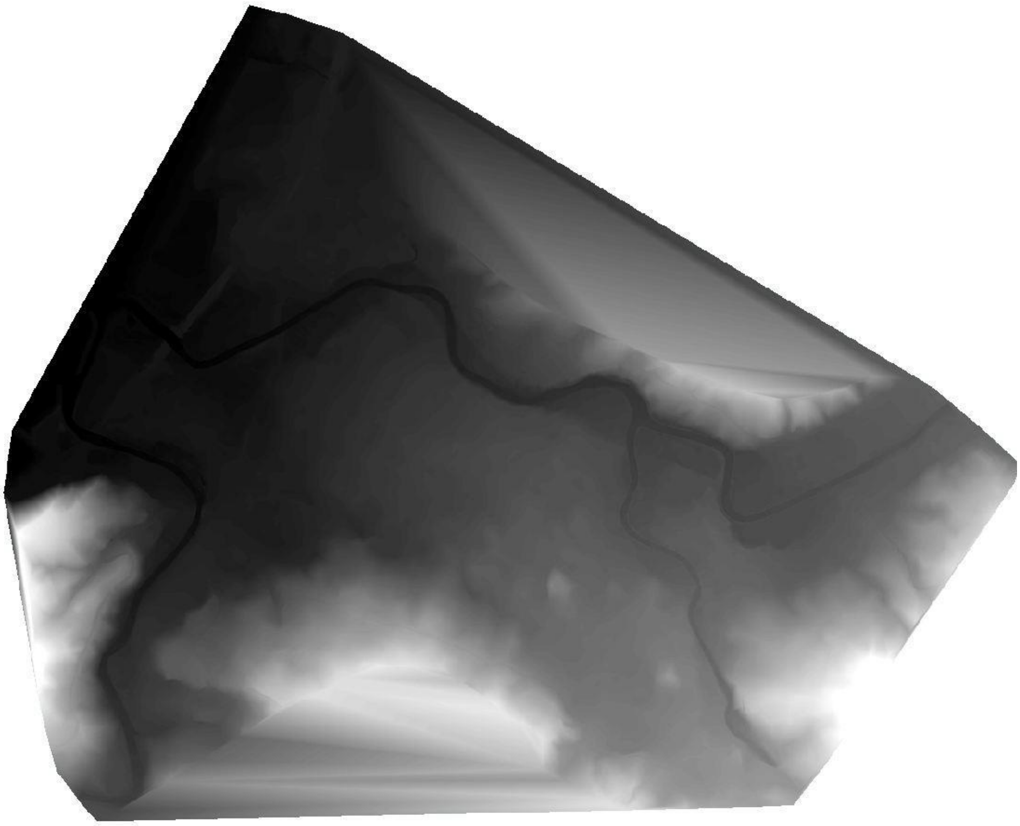

Figure 4.3: The Digital Elevation Model (DEM) (0.5 m x 0.5 m) created from the TIN.

4.1.3. Hydrological Data

The flood hydrographs for a 1 in 50 years flood event at the upstream of reaches have been considered as the upstream boundary conditions. The hydrographs for a Q_{50} flood event is provided in Table 4.1.

Table 4.1: The hydrographs for a Q_{50} flood event

t (hour)	Çam Creek (m^3/s)	Köprücü Creek (m^3/s)
0.5	5.6	5
1	17.4	18.4
1.5	49.2	53.9
2	94.7	99.5
2.5	126.2	118.8
3	128.2	113.2
3.5	126.2	109.5
4	127.8	113.6
4.5	127.6	109.8
5	111.5	90.8
5.5	88.7	67.8
6	65.5	48.2
6.5	48.6	35.4
7	37.2	26.7
7.5	28.8	19.7
8	22	15.3
8.5	17.3	12.2
9	14.2	10.3
9.5	12	8.5
10	10.2	7.6
10.5	8.9	6.7
11	8	5.9
11.5	7.3	5.6
12	6.5	5.4
12.5	6.2	5.3

Table 4.1 Continued

t (hour)	Çam Creek (m^3/s)	Köprücü Creek (m^3/s)
13	6.1	5
13.5	5.9	5
14	5.6	5

4.1.4. Reference Hydraulic Model Parameters

The model parameters used in the model such as Manning's n are collected from the site by analyzing soil samples in laboratories and rest of them were chosen within the suggested ranges from HEC-RAS technical manuals.

The two rivers are considered in three parts (codes that were used in analysis for the river part are given in parenthesis), first being Çam Creek Upstream (R1R1), the second one is Çam Creek Downstream (R1R1Low) and the third one is Köprücü Creek (R2R1). For each river, XSs at 4 m intervals are generated from TIN. The naming of XSs for each river parts is provided in Figure 4.4 and Table 4.2.

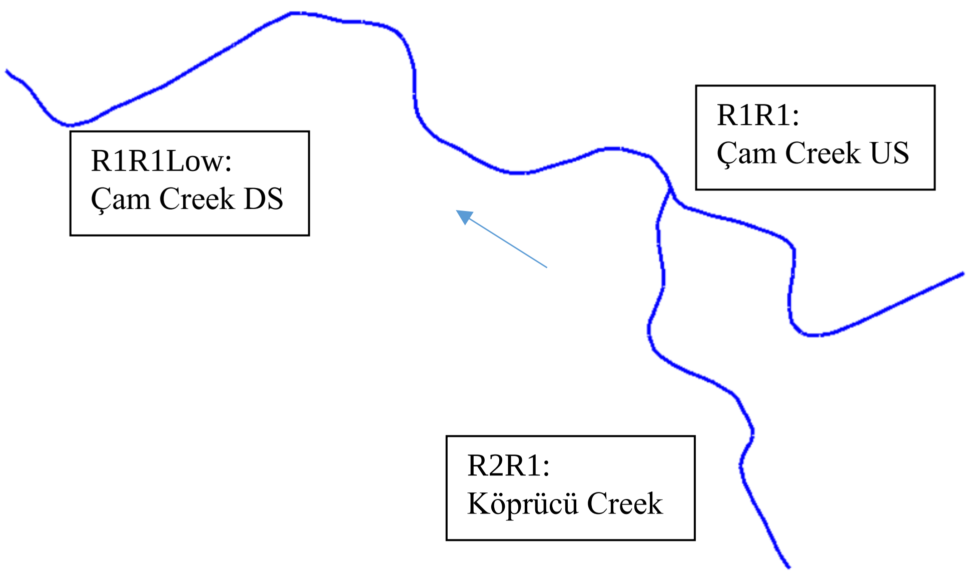

Figure 4.4: The river network with relevant coding and names.

Table 4.2: Names of the river network parts, XS stations and number of XSs.

River Name	XS (Upstream-Downstream)	# of XSs
Çam Creek Upstream	2077 - 1475	164
Çam Creek Downstream	1392 - 4	350
Köprücü Creek	760 - 40	183

The parameters of the reference model are provided in Table 4.3 and Table 4.4. The Manning's n parameters are considered in 4 sections (M1...M4) since the riverbed characteristics vary along the river network.

Table 4.3: The Manning's n coefficients values of the reference model throughout the river network

	M1: Çam Cr. US (R1R1)	M2: Çam Cr, DS (R1R1Low) (XSs 1304-784)	M3: Çam Cr. DS (R1R1Low) (XSs 780-4)	M4: Köprücü Cr. (R2R1)
Manning's n	0.038	0.038	0.046	0.044

Table 4.4: The reference model parameter values of four remaining parameters

Normal Depth (DS BC)	0.0105
Drag Coefficient for Bridges	1.2
Weir Coefficient for Bridge Decks	1.4
Weir Coefficient for Lateral Structures	1.1

4.2. Results of Random Number Generation for Five Parameters

A code that utilizes Box-Muller transformation method was used to generate the random numbers for each error source. The number of values (see Table 1.1), estimated variations (explained in the following subchapters) in the form of standard deviation and mean values (the parameters of reference model) (see Table 4.3 and Table 4.4) are defined within the code.

4.2.1. Manning's n coefficient

Even if all the measures in assigning Manning's roughness coefficient are taken, due to the complexity of the parameter in terms of vertical-horizontal variations and irregularities throughout the riverbed, it is likely that Manning's n coefficient is one of the major error sources. This assumption is made assuming that the modeler is experienced enough and input parameters, such as topographical data and hydrological data are reliable. Studies from Özbey (2012) and Goodell (2014) show that even the best approximation in the coefficient can be in error as high as ±25%. Therefore, a 25% range of standard deviation is assigned for the random number generation procedure, which is used later on to generate the models. The charts of generated values of four Manning's n regions by utilizing the Box Muller transformation algorithm are provided in Figure 4.5 to Figure 4.8 along with statistical summary data of generated values provided in Table 4.5.

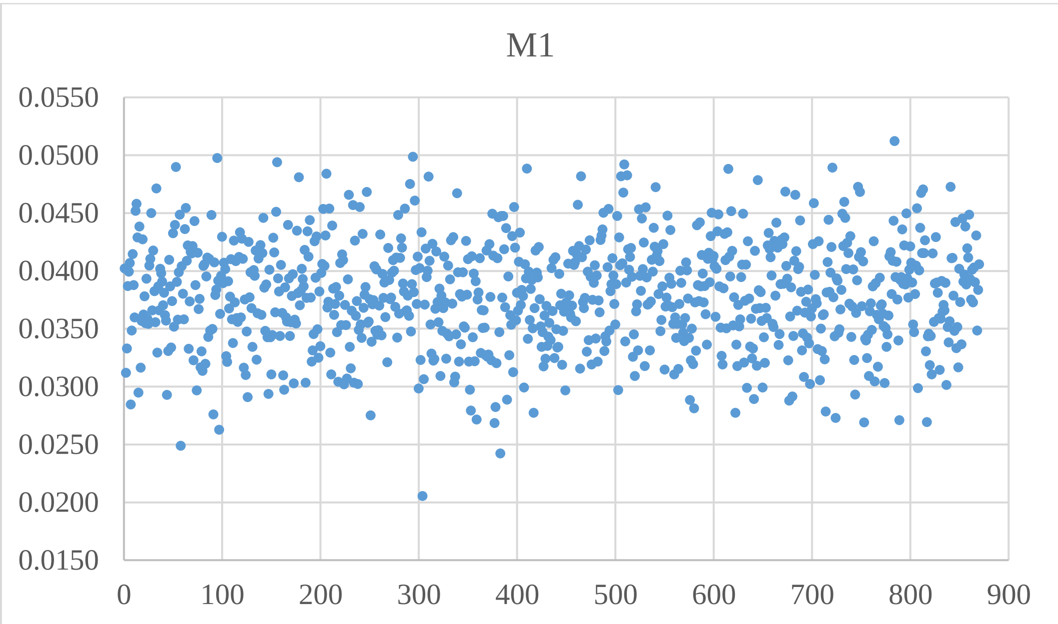

Figure 4.5: Distribution chart of generated values for M1 region.

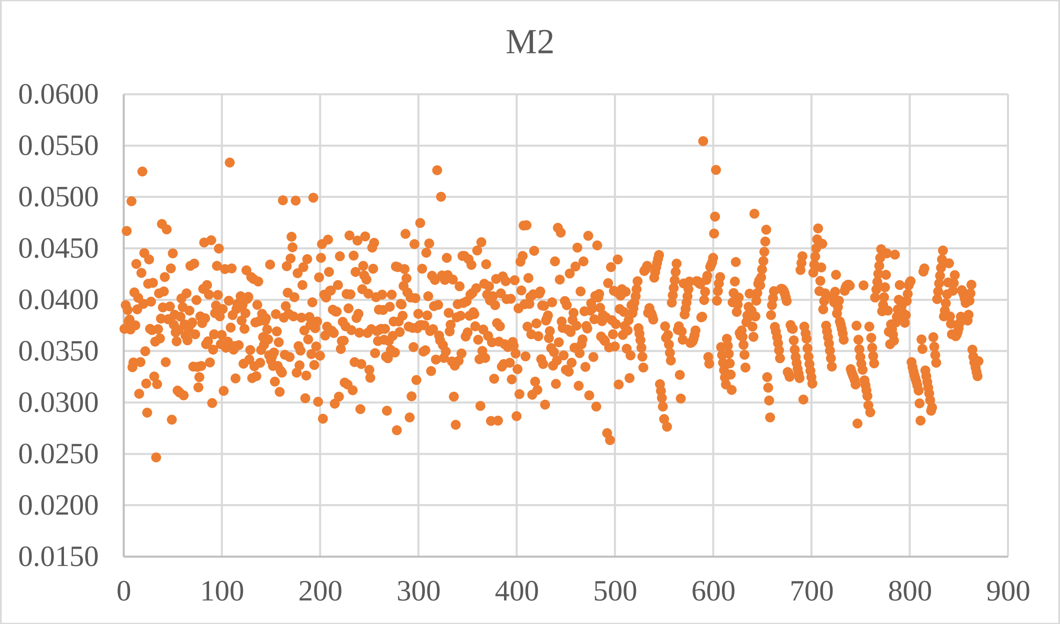

Figure 4.6: Distribution chart of generated values for M2 region.

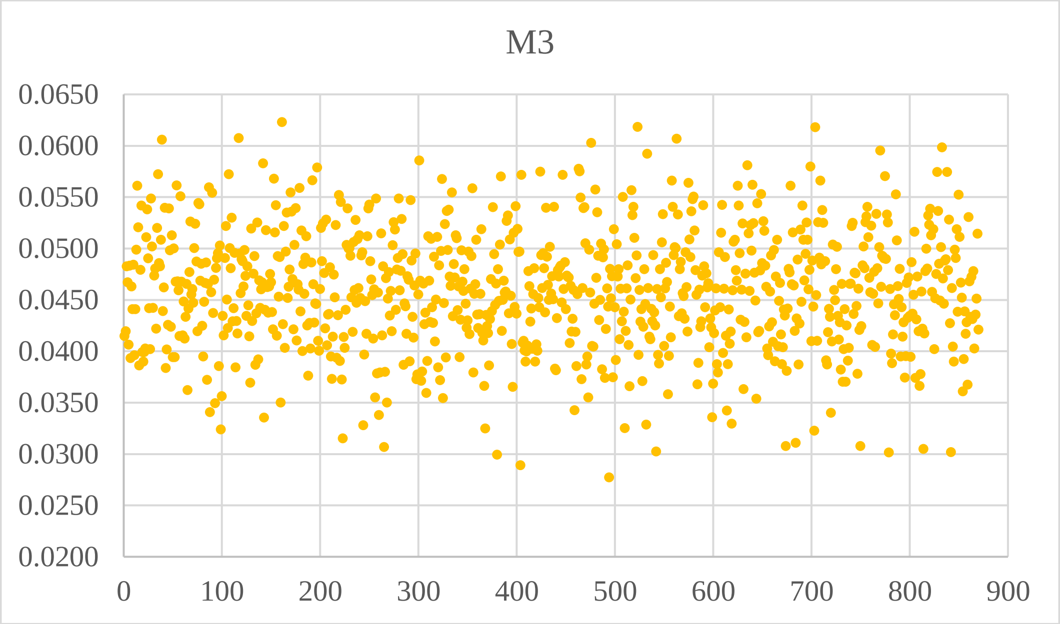

Figure 4.7: Distribution chart of generated values for M3 region.

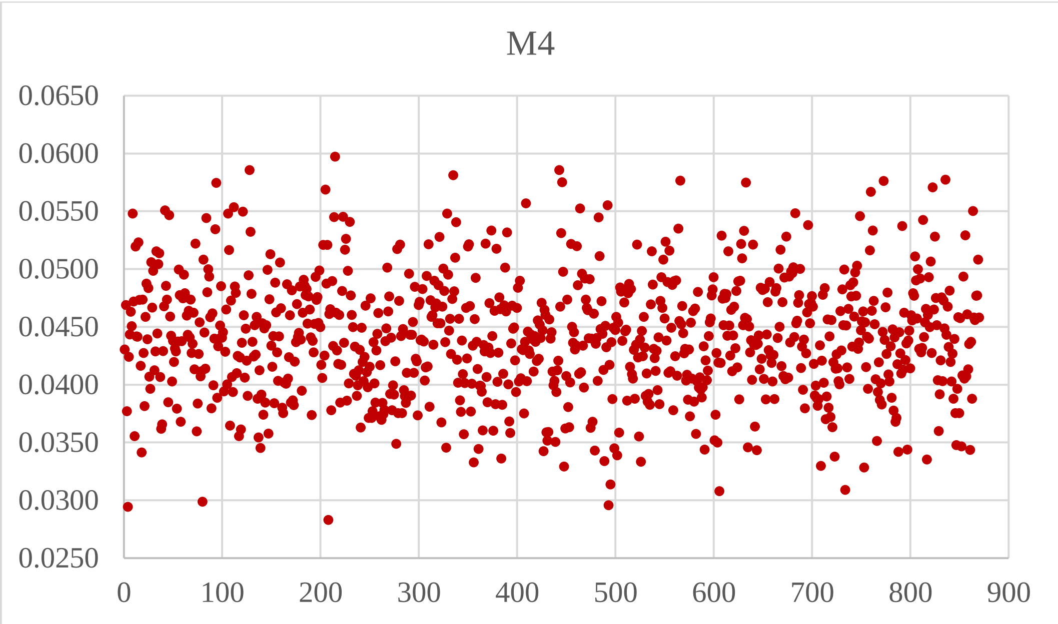

Figure 4.8: Distribution chart of generated values for M4 region.

Table 4.5: Statistical summary table of 4 regions of generated values Manning's n data.

Statistical Summary	*M1*	*M2*	*M3*	*M4*
Mean	0.037915	0.038041	0.045921	0.044007
Standard Error	0.000155	0.000149	0.000197	0.000174
Median	0.037881	0.038	0.046039	0.043934
Mode	0.035659	0.04303	0.054166	0.044174
Standard Deviation	0.004577	0.004404	0.005809	0.00513
Sample Variance	2.09E-05	1.94E-05	3.37E-05	2.63E-05
Kurtosis	0.01237	0.321367	0.055105	0.132483
Skewness	-0.07345	0.139346	-0.07469	0.140281
Range	0.030666	0.030778	0.034556	0.031401
Minimum	0.020546	0.024652	0.027727	0.028303
Maximum	0.051212	0.05543	0.062283	0.059704
Count	870	870	870	870

4.2.2. Normal Depth (Friction Slope) as Downstream Boundary Condition

Downstream boundary condition can often be a source of model error and a cause for instability. Most of the time, the true stage for a given flow at the downstream end is unknown. Within the study the downstream condition of the river system is assumed to be normal depth for manageability of the error sources. HEC-RAS requires the user to enter a single energy slope to compute the downstream stage for any flow occurring. It is estimated that a reliable approximation of Normal Depth parameter may result in an error as high as ±15%. The chart of generated values of Normal Depth (Friction Slope) by utilizing the Box Muller transformation algorithm is provided in Figure 4.9 along with statistical summary data of generated values provided in Table 4.6.

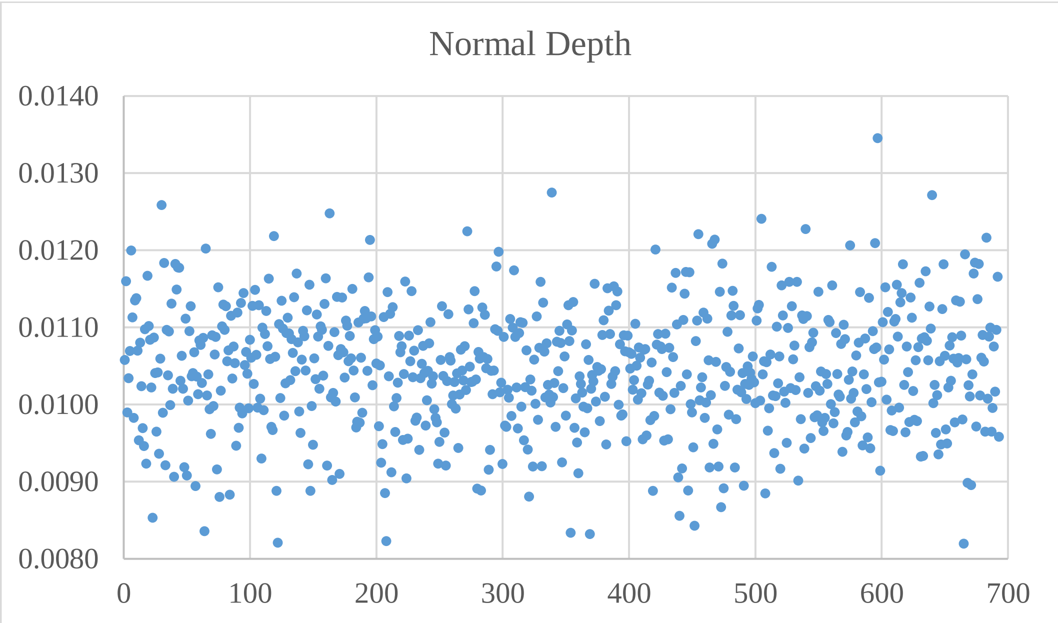

Figure 4.9: Distribution chart of generated values for Normal Depth parameter.

Table 4.6: Statistical summary table of generated values for Normal Depth parameter.

Statistical Summary	*Normal Depth*
Mean	0.01045
Standard Error	2.99705E-05
Median	0.010436
Mode	0.010968
Standard Deviation	0.000789
Sample Variance	6.22475E-07
Kurtosis	0.234778
Skewness	-0.02487
Range	0.005257
Minimum	0.008198
Maximum	0.013455
Count	693

4.2.3. Drag Coefficient for Bridges

Drag coefficients are used to estimate the force due to the water moving around piers, the separation of the flow, and the resulting wake that occurs downstream. It is considered as a potential error source especially at the upstream of the bridges with piers. The chart of generated values of Drag coefficient by utilizing the Box Muller transformation algorithm is provided in Figure 4.10 along with statistical summary data of generated values provided in Table 4.7.

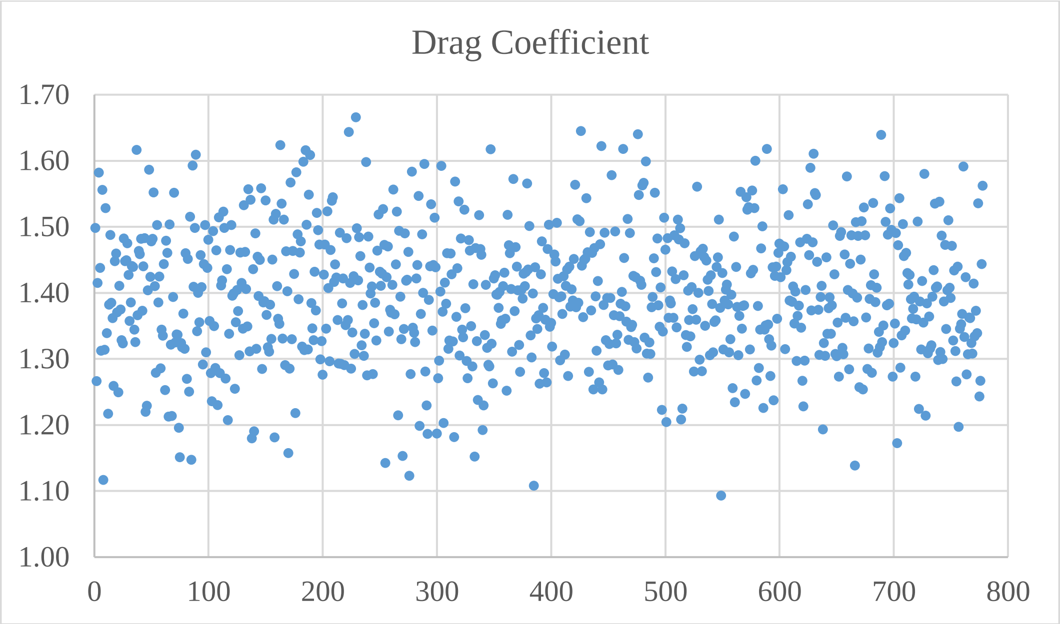

Figure 4.10: Distribution chart of generated values for Drag coefficient.

Table 4.7: Statistical summary table of generated values for Drag coefficient.

Statistical Summary	*Drag Coefficient*
Mean	1.39545
Standard Error	0.00357
Median	1.39379
Standard Deviation	0.09971
Sample Variance	0.00994
Kurtosis	-0.0817
Skewness	-0.0343
Range	0.57264
Minimum	1.09282
Maximum	1.66546
Count	778

4.2.4. Weir Coefficient for Bridge Decks

In the work of Brater, King, Lindell and Wei (1996), the parameter value variation of broad crested weir is given between 1.38 – 1.71, which is under free flow conditions where the discharge is independent of tail water. However, having very little experimental data on the behavior of bridge decks during a flood event, it is certain that obstructions, such as the debris stuck on the downstream side of the bridge, likely decrease the discharge coefficient. In such cases, it is recommended that the bridge weir coefficients should be taken as 1.44 (Bradley, 1960). The error in the assigned weir coefficient is assumed to be as high as 25 percent. The chart of generated values of Bridge Weir coefficient by utilizing the Box Muller transformation algorithm is provided in Figure 4.11 along with statistical summary data of generated values provided in Table 4.8.

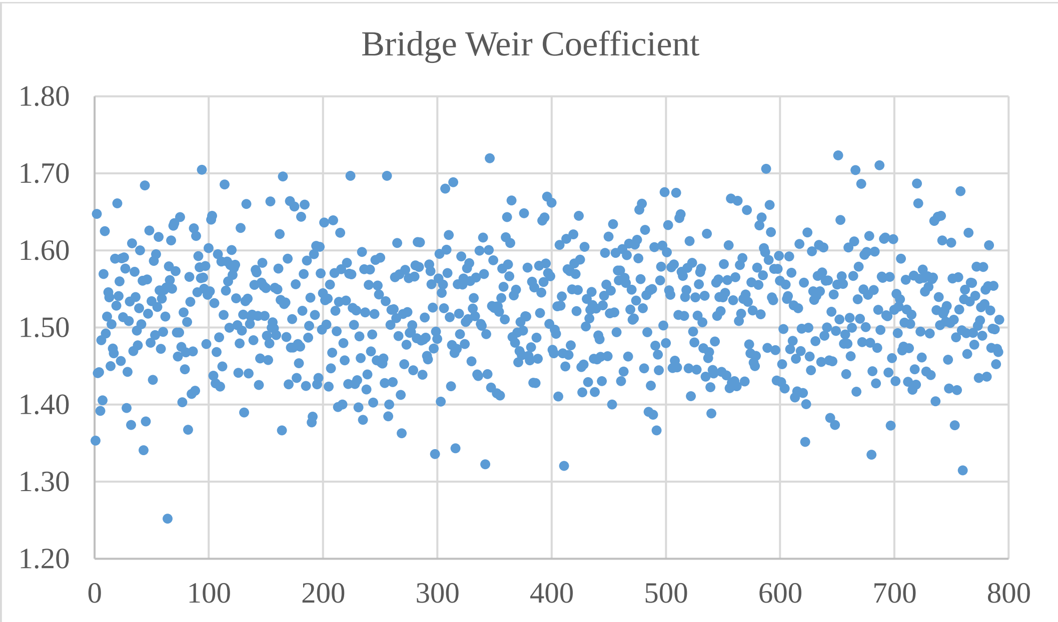

Figure 4.11: Distribution chart of generated values for Bridge Weir coefficient.

Table 4.8: Statistical summary table of generated values for Bridge Weir coefficient.

Statistical Summary	*Bridge Weir Coef.*
Mean	1.52332
Standard Error	0.00260
Median	1.52478
Standard Deviation	0.07341
Sample Variance	0.00539
Kurtosis	-0.01735
Skewness	-0.05771
Range	0.47149
Minimum	1.25189
Maximum	1.72338
Count	792

4.2.5. Weir Coefficient for Lateral Structures

The lateral weirs that connect 1D hydraulic components to 2D hydraulic components are considered an error source. The lateral weir coefficient may change with due to the shape of the weir (which is rarely consistent and regular), the angle of the curb of the riverbed, etc. The table for possible lateral weir coefficients is provided in "HEC-RAS 2D Modeling User's Manual" (Brunner, 2016c) (see Table 4.9). The error in assigning the coefficient for the lateral weir in this study is assumed to be as high as ±25%. The chart of generated values of Lateral Weir coefficient by utilizing the Box Muller transformation algorithm is provided in Figure 4.12 along with statistical summary data of generated values provided in Table 4.10.

Table 4.9: Lateral weir coefficients (Brunner, 2016c).

What is being modeled with the Lateral Structure	**Description**	**Range of Weir Coefficients**
Levee/Roadway - 3ft or higher above natural ground	Broad crested weir shape, flow over levee/ road acts like weir flow	SI Units: **0.83** to **1.43**

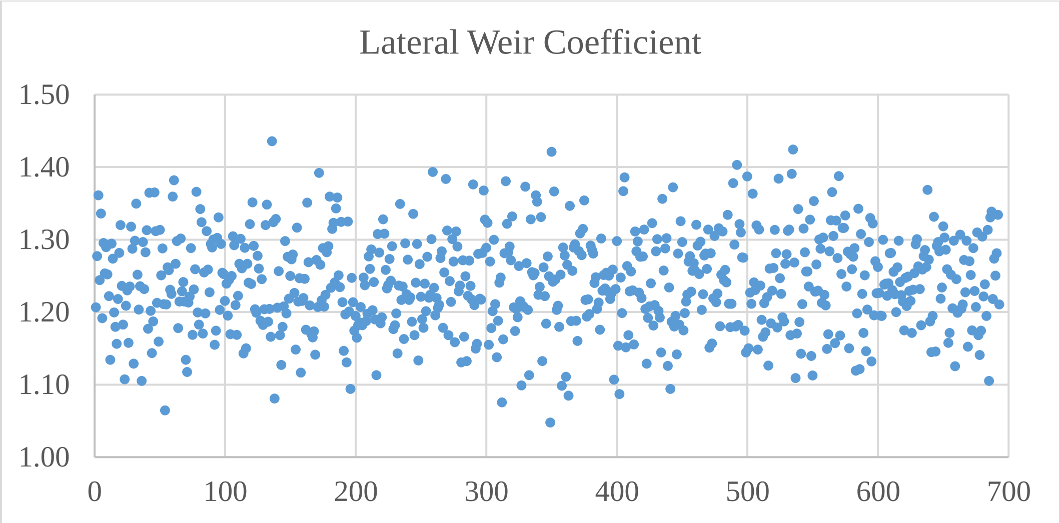

Figure 4.12: Distribution chart of generated values for Lateral Weir coefficient.

Table 4.10: Statistical summary table of generated values for Lateral Weir coefficient.

Statistical Summary	*Lateral Weir coefficient*
Mean	1.24093
Standard Error	0.00248
Median	1.23884
Mode	1.28072
Standard Deviation	0.06538
Sample Variance	0.00427

Table 4.10 Continued

Statistical Summary	*Lateral Weir coefficient*
Kurtosis	-0.176
Skewness	0.0512
Range	0.38808
Minimum	1.04731
Maximum	1.43539
Count	693

4.3. Results of Model Runs

The results of the generated hydraulic model runs are the data that is used to construct the uncertainty budgets. Therefore, a detailed evaluation of the data was conducted. The maximum and minimum values that lied beyond the reasonable resulting data range were eliminated. The data was also evaluated to assess in order to determine which distribution is the best fit to express it. 16 XSs out of 684 and 14 2D cells out of 3825 which shows the largest standard deviation in the dataset are presented in this study to demonstrate the likely values of combined uncertainties. A representative figure to show the cross section and 2D computational cell structures and naming are given in Figure 4.13. The resulting profiles and inundation map of the hydraulic model is given in Figure 4.14 and Figure 4.15. The detailed explanations are provided in the subchapters along with frequency analysis of datasets which are provided in Figure 4.16, Figure 4.17 and Figure 4.18 along with statistical summaries given in Table 4.11, Table 4.12, Table 4.13 and Table 4.14.

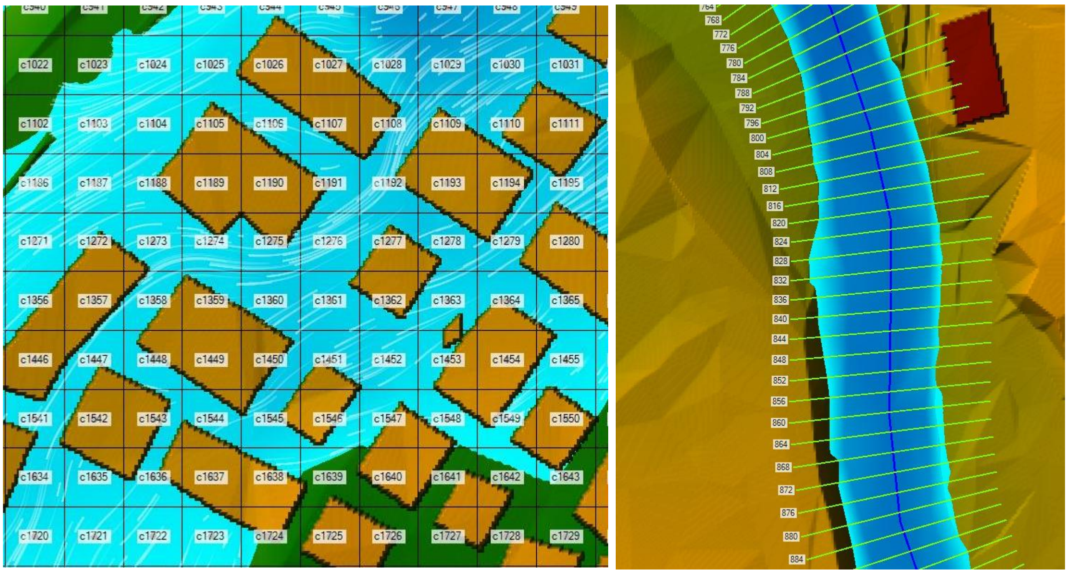

Figure 4.13: Resulting profile of the reference hydraulic model

5 different relatively identical computers which was equipped with hardware of Intel® Core™ i7 processor and 8 to 64 GB RAM were used to run the models simultaneously. Each generated hydraulic model took an average of 30 minutes (varies between 27 to 35 min.) to run, therefore for each computer it took about 16 days (22,950 min) of non-stop computing for all the simulations to finish.

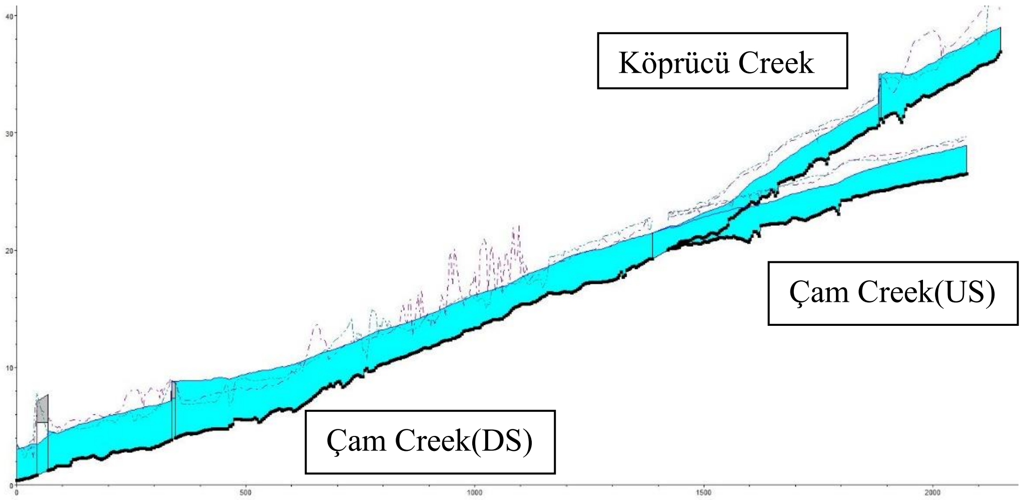

Figure 4.14: Resulting profile of the reference hydraulic model (x axis: station in meters; y axis: elevation in meters)

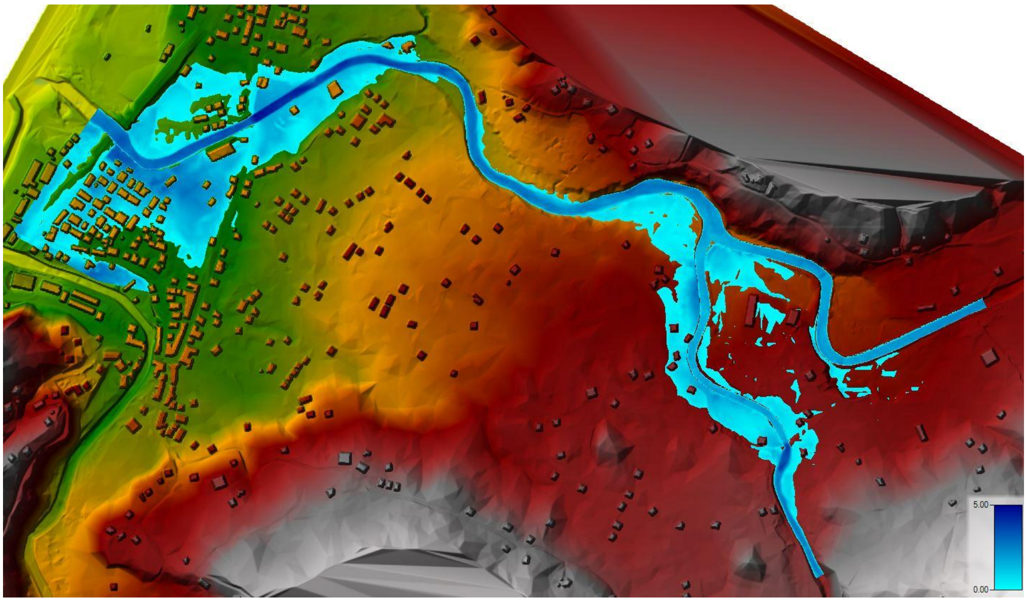

Figure 4.15: Resulting inundation map (depth) of the hydraulic model

4.3.1. Resulting MWSEs due to Manning's n variation

The figure below represents the frequency analysis of the resulting MWSEs on XS 724 placed in Çam Creek Downstream (coded as R1R1Lower) due to Manning's n variations of a total of 870 model runs. This XS is provided as an example because the variance in the data are significant. The statistical summary tables below aims to show the statistical properties of the resulting data as well as to show the data is a fit for Gaussian distribution.

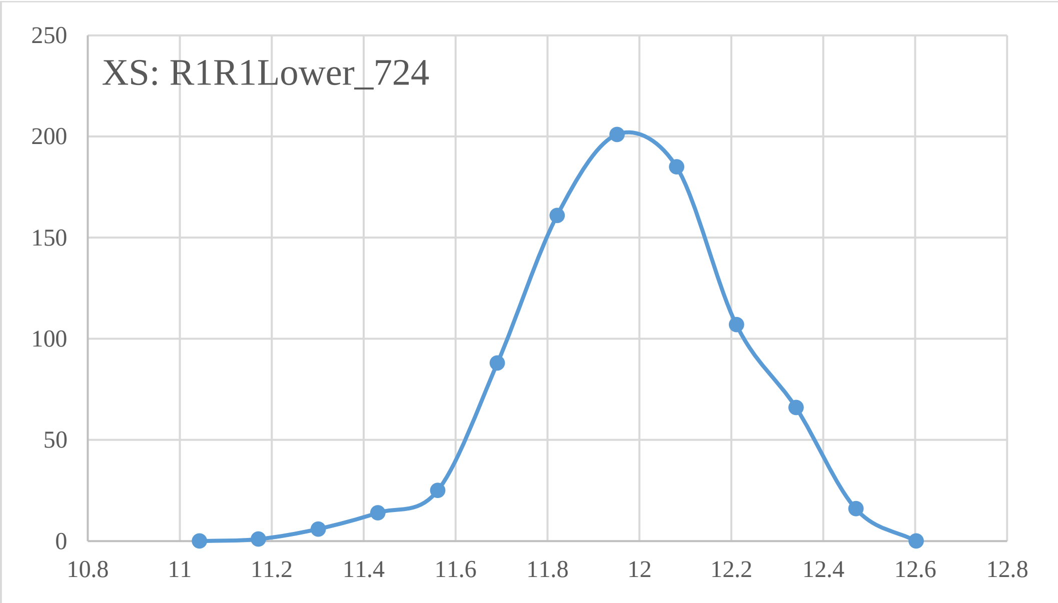

Figure 4.16: Frequency analysis of XS R1R1Lower_724 for the generated model of variations of Manning's n.

Having mean and median values very close to each other along with Kurtosis and Skewness values between -2 and 2 strongly indicates that the error distribution of the data is Gaussian distribution. As provided in Table 4.11, Table 4.12 and Table 4.13; the datasets indicates properties of Gaussian distribution.

Table 4.11: Statistical summary table of XS R1R1Lower_724.

Statistical Summary	*R1R1Lower_724(Manning's n)*
Mean	11.91121
Standard Error	0.0075
Median	11.9162
Mode	11.7567
Standard Deviation	0.22144
Sample Variance	0.04904
Kurtosis	0.04237
Skewness	-0.20858
Range	**1.2995**
Minimum	11.1713
Maximum	12.4708
Count	870

4.3.2. Resulting MWSEs due to Normal Depth variation

The figure below represents the frequency analysis of the resulting MWSEs on XS 4 placed in Çam Creek Downstream (coded as R1R1Lower) due to Normal Depth parameter variations of a total of 693 model runs. This XS is provided as an example because the variance in the data are significant.

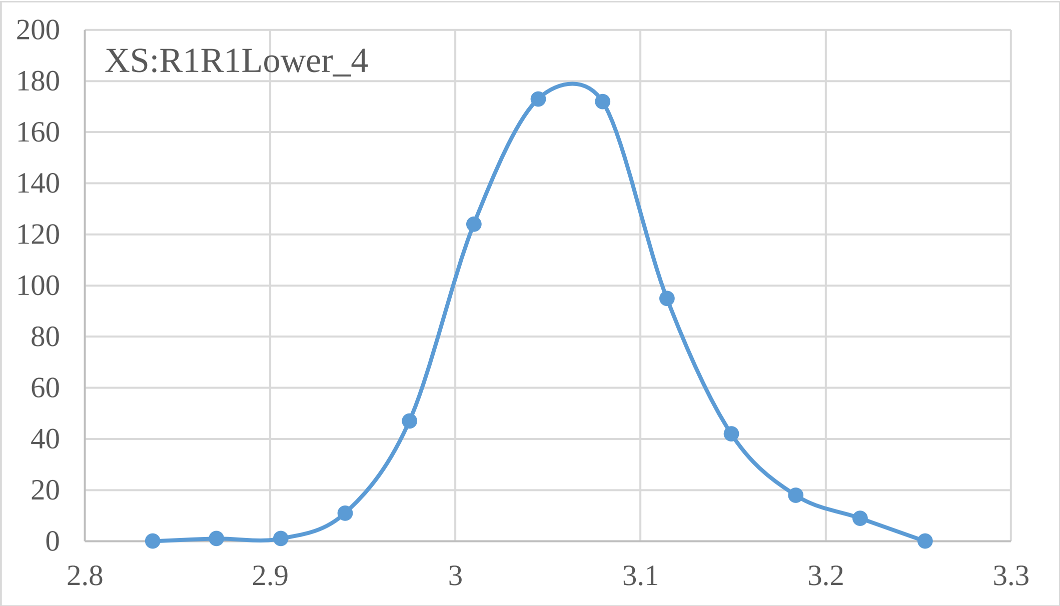

Figure 4.17: Frequency analysis of XS R1R1Lower_4 for the generated model of variations of Normal Depth.

Table 4.12: Statistical summary table of XS R1R1Lower_4.

Statistical Summary	*R1R1Lower_4 (Normal Depth)*
Mean	3.0447
Standard Error	0.00205
Median	3.04349
Mode	3.04805
Standard Deviation	0.054
Sample Variance	0.00292

Table 4.12 Continued

Statistical Summary	*R1R1Lower_4 (Normal Depth)*
Kurtosis	0.32156
Skewness	0.34072
Range	**0.34759**
Minimum	2.87095
Maximum	3.21854
Count	693

4.3.3. Resulting MWSEs due to lateral weir coefficient variation

The figure below represents the frequency analysis of the resulting MWSEs on XS 527 placed in Köprücü Creek (coded as R2R1) due to lateral weir coefficient variations of a total of 692 model runs. This XS is provided as an example because the variance in the data are significant.

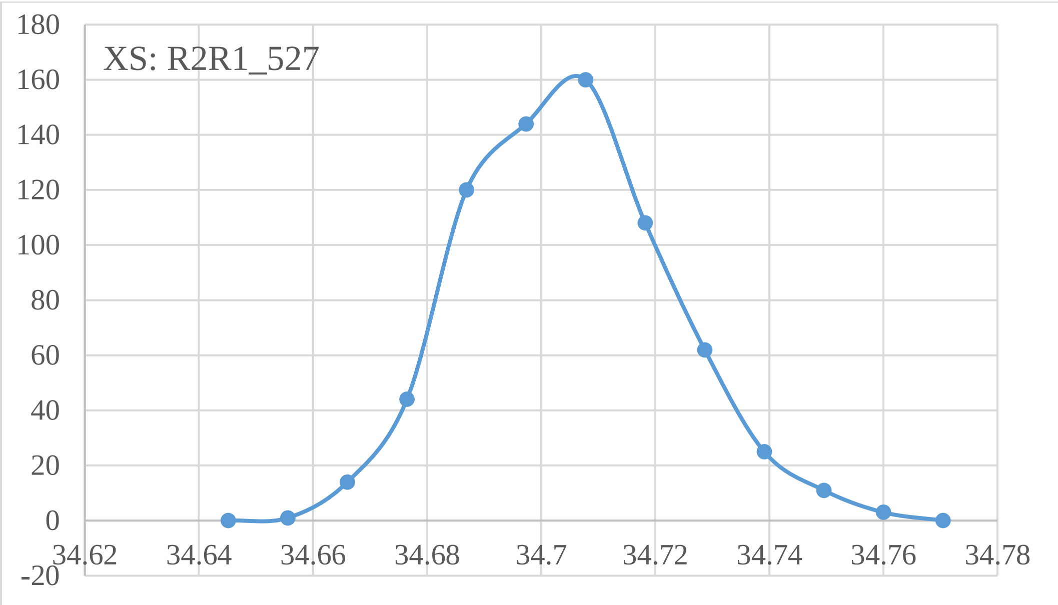

Figure 4.18: Frequency analysis of XS R2R1_527 for the generated model of variations of Lateral Weir.

Table 4.13: Statistical summary table of XS R2R1_527.

Statistical Summary	*R2R1_527 (Lateral Weir)*
Mean	34.6993
Standard Error	0.00067
Median	34.6993
Mode	34.6876
Standard Deviation	0.01758
Sample Variance	0.00031
Kurtosis	-0.0792
Skewness	0.29936
Range	**0.1044**
Minimum	34.6556
Maximum	34.76
Count	692

4.3.4. Resulting MWSEs due to Bridge Drag and Weir coefficient variation

The statistical summary table for both parameters are given on the Table 4.14. The results for variations of bridge drag and weir coefficients do not indicate a normal distribution, therefore the standard deviations are misleading, however the ranges –specified with bold- indicates that the impacts of these two parameters are almost negligible, the ranges between the minimum and maximum values caused by the variation of these parameters on MWSE are 7 cm for drag coefficient and 10 cm for weir coefficient whereas the range caused by Manning's n variation on MWSEs are as high as 1.3 m (Table 4.11). Therefore, these results will be included, although with minimal impact, to the uncertainty budget as though it fits Gaussian distribution.

Table 4.14: Statistical summary table of XS R1R1Lower_76 (drag coefficient) and R2R1_500 (weir coefficient).

Statistical Summary	*Drag Coefficient*	*Weir Coefficient*
Mean	4.57585	34.6207
Standard Error	0.00061	0.00126
Median	4.58122	34.6392
Mode	4.58346	34.6408
Standard Deviation	0.01703	0.03552
Sample Variance	0.00029	0.00126
Kurtosis	4.35936	-0.14774
Skewness	-2.46120	-1.33235
Range	**0.06963**	**0.0943**
Minimum	4.51944	34.5503
Maximum	4.58907	34.6446
Count	778	791

4.4. The Combined Uncertainty Budget

The uncertainty budgets of 16 XSs and 14 2D cells are constructed within the study. The selection of the XSs and 2D cells, that the uncertainty budgets calculations were based on, are the points where the largest variation (larger standard deviation) in the data are observed. The remaining XS and 2D cells are picked randomly within the transition region between maximum standard deviation values. The example calculation tables are given in Table 4.15 and Table 4.16, the summary table of results for XS and 2D cells are given in Table 4.17 and Table 4.18; the results of all calculation tables for 16 XSs and 14 2D cells are provided in the Appendices. It was found that the bridge drag and weir coefficients have minimal effect on the uncertainty budget, therefore these datasets were not included in the 2D cell uncertainty budget calculations.

As provided in Table 4.15, the standard deviation, $u(x_i)$, of the data caused by the variation of each error sources, the degree of freedom, v, the sensitivity coefficients c and coverage factor k are the major inputs of calculations. Then these values are combined using ISO GUM method described in Chapter 3.2.1 to find the resulting combined uncertainty. The equations numbers given in Chapter 3.2.1 are shown in Table 4.15 adjacent to the corresponding calculations. The combined uncertainty budget for XS 2053 on Çam Creek US is ± 0.3427 m at 95% confidence level with coverage factor of 1.96 (Table 4.15).

For this study, an extensive dataset of 3,825 models were generated for which maximum Water Surface Elevation data of 684 XSs and 7139 2D computational cells were analyzed. Eventually, uncertainty budgets for 16 selected XSs and 14 selected 2D cells were calculated. It is seen that the variations in input parameters result in a maximum combined uncertainty of ± 0.454 m (Table 4.17) for cross sections and ± 0.664 m (Table 4.18) for 2-dimensional computational cells at 95% confidence level with coverage factor for the interval of 1.96. The uncertainty budget indicates that the MWSE is expected to change as much as 16% in XSs. It would be safe to say that the majority of the error is due to the variation in Manning's n coefficient while the Normal Depth variation affect the downstream region as expected; the impact of Lateral Weir, Bridge Drag and Bride Weir coefficients are minor.

Table 4.15: Example of an Uncertainty Budget calculation of XS 2053 at Çam Creek Upstream.

R1R1_2053	Component Values						
Uncertainty Components	U_i	k_i	$u(x_i)$	c_i	$\|c_i.u(x_i)\|$	v_i	$\|c_i.u(x_i)\|^4/v_i$
1. Manning n coefficient ±25%	0.342234568	1.96	0.1746095	1	0.174609474	872	1.06599E-06
2. Downstream Boundry Condition ±15%	6.96835E-15	1.96	3.555E-15	1	3.55528E-15	692	2.30881E-61
3. Lateral Weir Coefficient ±25%	6.96836E-15	1.96	3.555E-15	1	3.55528E-15	691	2.31217E-61
4. Drag Coefficient of Bridges ±25%	2.64776E-13	1.96	1.351E-13	1	1.3509E-13	777	4.28619E-55
5. Bridge Weir Coefficient ±25%	2.99612E-13	1.96	1.529E-13	1	1.52863E-13	791	6.90296E-55
				Σu_i^2**(2)**=	0.030488468	Σ=	1.06599E-06
				u_c**(3)**=	0.174609474		
				u_c^4=	0.000929547	v_{eff}**(5)**=	872
						k **(6)**=	1.9629
			Max WSE=	28.7 m	*U* **(4)**@.95% Conf. Lev. =		**±0.3427**

Table 4.16: Example of an Uncertainty Budget calculation of 2D Cell values for Perimeter 1 - Cell 78.

P1_7	Component Values						
Uncertainty Components	U_i	k_i	$u(x_i)$	c_i	$\|c_i.u(x_i)\|$	v_i	$\|c_i.u(x_i)\|^4/v_i$
1. Manning n coefficient ±25%	0.51560415	1.96	0.26306334	1	0.2630633	870	5.50455E-06
2. Downstream Boundry Condition ±15%	4.87784E-13	1.96	2.4887E-13	1	2.489E-13	692	5.54346E-54
3. Lateral Weir Coefficient ±25%	0.039581206	1.96	0.02019449	1	0.0201945	592	2.80938E-10
				Σu_i^2=	0.0696101	Σ=	5.50483E-06
				u_c=	0.2638373		
				u_c^4=	0.0048456	v_{eff}=	880.2393167
						k=	1.9628
			Max WSE=	23.5 m	*U* @.95% Conf. Lev. =		**±0.5179**

Table 4.17: Estimated Maximum Water Surfaces and combined expanded uncertainties at 95% confidence level at the selected XS located in the river network.

Code of the XS	Maximum Water Surface ± Uncertainity at 95% Conf. Level (m)
Çam Creek US	
R1R1_2053	28.696±0.343
R1R1_1765	25.43±0.309
R1R1_1569	23.504±0.34
R1R1_1429	21.883±0.162
Çam Creek DS	
R1R1Low_1324	20.704±0.319
R1R1Low_1160	18.513±0.262
R1R1Low_580	9.875±0.23
R1R1Low_340	7.107±0.326
R1R1Low_140	**5.161 ± 0.454**
R1R1Low_72	4.545 ± 0.302
R1R1Low_4	3.034 ± 0.359
Köprücü Creek	
R2R1_696	37.629 ± 0.284
R2R1_500	34.555 ± 0.092
R2R1_404	30.448 ± 0.242
R2R1_132	23.385 ± 0.234
R2R1_44	22.021 ± 0.137

Table 4.18: Estimated Maximum Water Surfaces and combined expanded uncertainties at 95% confidence level at the selected Cells located through 2D Flow Areas.

Code of the Cell	Maximum Water Surface ± Uncertainity at 95% Conf. Level (m)
Perimeter 1	
P1_7	23.505 ± 0.518
P1_78	23.505 ± 0.482
P1_109	23.505 ± 0.38
P1_1158	23.505 ± 0.504
Perimeter 2	
P2_30	11.824 ± 0.392
P2_85	9.576 ± 0.277
P2_461	7.734 ± 0.068
P2_2705	11.507 ± 0.432
P2_2766	5.981 ± 0.062
Perimeter 3	
P3_428	13.274 ± 0
P3_712	10.489 ± 0.395
P3_1013	8.851 ± 0.304
P3_1456	**14.536 ± 0.664**
P3_1751	16.418 ± 0.204

CHAPTER 5

SUMMARY AND CONCLUSION

Within the scope of this study, five possible error sources in a hydraulic model are analyzed to construct uncertainty budgets. A reference model derived from a case study in Kemalpaşa, Artvin, Turkey was treated as a laboratory to quantify the combined uncertainty of the variance of 5 error sources, namely the Manning's n coefficient, Normal Depth (friction slope), drag coefficient for bridges, weir coefficient for bridge decks and weir coefficient for lateral structures. A total of 3825 models are generated with randomly generated values of error sources using customized VBA codes. The models results are exported using a Python code and analyzed in Microsoft Excel sheet. Utilizing the results data of MWSE of 684 XSs and 7139 2D computational cells, the ISO GUM approach applied to find combined uncertainties of the XS and 2D computational cells that shows the maximum variance along with other random XS and 2D computational cells.

It is clear that this study does not reflect a complete uncertainty budget of a 1D&2D hydraulic model. There are many aspects such as the sea river interaction, topographical data, hydrological data and other hydraulic parameters to be considered. However, this study presents a clear framework for future works that deals with extended error sources.

The study gives a clear picture of the need in engineering studies of an approach of expressing the results with uncertainty measures. Expressing the combined uncertainties would give the decision maker the opportunity of seeing the minimum and maximum extends of results. It will be beneficial to express the quality of the study as well as to justify the economical aspect of the decisions. The decision makers and engineers may decide to adjust the design criteria according to resulting combined uncertainties and approach for more economically efficient projects. Most importantly, this study provides an approach to how to calculate the possible errors that the decision makers and engineers should always consider along with provided results.

The possibilities of interpretation of results with such detail and context are widely varied. It should be noted that the uncertainty concept and statistical analysis of it is yet a young science. It is certain that the scientists, engineers and decision maker will be using the language of uncertainty rather than the determinist language more frequently in the future.

REFERENCES

Bell, S. (1999). *A Begginer's Guide to Uncertainty of Measurement.* Middlesex, UK: National Physical Laboratory.

Bentley, R. E. (2005). *Uncertainty In Measurement: The ISO Guide - Monograph 1.* Lindfield NSW, Australia: National Measurement Institute.

Bradley, J. N. (1960). *Hydraulics of Bridge Waterways - Hydraulic Design Series No.1.* Washington: U.S. Department of Commerce Bureau of Public Roads.

Brater, E., King, H. W., Lindell, J. E., & Wei, C. Y. (1996). *Handbook of Hydraulics for the Solution of Engineering Problems.* Boston: McGraw-Hill.

Brunner, G. W. (2016a). *HEC-RAS River Analysis System Hydraulic Refence Manual Version 5.0.* Davis, California: USACE Hydraulic Engineering Center.

Brunner, G. W. (2016b). *HEC-RAS River Analysis System User's Manual Version 5.0.* Davis: USACE Hydralic Engineering Center (HEC).

Brunner, G. W. (2016c). *HEC-RAS River Analysis System, 2D Modeling User's Manual Version 5.0.* Davis: USACE Hydraulic Engineering Center (HEC).

Brunner, G., Piper, S. S., Jensen, M. R., & Chacön, B. (2015). Combined 1D and 2D Hydraulic Modeling within HEC-RAS. *World Environmental and Water Resources Congress.*

Casulli, V. (2009), A high-resolution wetting and drying algorithm for free-surface hydrodynamics. Int. J. Numer. Meth. Fluids, 60: 391-408. doi:10.1002/fld.1896

Chacön, B., Faber, B. A., DeGeorge, J. F., & Fleming, M. J. (2014). Columbia River Treaty 2014/2024: Monte Carlo Simulation in HEC-WAT. *World Environmental and Water Resources Congress* .

Deardorff, D. L. (2001). *Introductory Physics Students' Treatment of Measurement Uncertainty.* Raleigh: North Carolina State University.

EPA. (2004, July). MARLAP Manual Volume III: Chapter 19, Measurement Uncertainty. USA.

Goodell, C. (2013, April 9). *HEC-RAS File Types*. The Ras Solution: Retrieved from http://hecrasmodel.blogspot.com/2013/04/hec-ras-file-types.html

Goodell, C. (2014). *Breaking The HEC-RAS Code - A User Guide to Automating HEC-RAS.* Portland: h2ls.

JCGM. (2008). *Evaluation of measurement data - Guide to the expression of uncertainty in measurement.* Switzerland.

Oubennaceur, K., Chokmani, K., Nastev, M., Tanguy, M., & Raymond, S. (2018). Uncertainty Analysis of a Two-Dimensional Hydraulic Model. *Water*.

Ozbey, N. (2012). Acoustic Doppler Technology and Estimating Manning Roughness Coefficients from Nikuradse's Equivalent Sand Roughness. *Hydrology and Water Reource Symposium.* Australia.

SATLAB Geosolutions. (2014). *SL500 Technical Manual.* Sweden.

Thomas, D. B., Luk, W., Leong, P. H., & Villasenor, J. D. (2007). Gaussian Random Number Generators. *ACM Computing Surveys, 39*(4), Article 11. doi:10.1145/1287620.1287622

Wikipedia. (2019, 07 03). *Box–Muller transform*. Retrieved from Wikipedia: https://en.wikipedia.org/wiki/Box%E2%80%93Muller_transform

APPENDICES

A. Uncertainty Budget Tables of Selected Cross Sections

Table A 1: Calculation table of XS 2053 on Çam Creek Upstream

R1R1_2053	Component Values						
Uncertainty Components	U_i	k_i	$u(x_i)$	c_i	$\|c_i.u(x_i)\|$	v_i	$\|c_i.u(x_i)\|^4/v_i$
1. Manning n coefficient ±25%	0.342234568	1.96	0.1746095	1	0.1746095	872	1.06599E-06
2. Downstream Boundry Condition ±15%	6.96835E-15	1.96	3.555E-15	1	3.555E-15	692	2.30881E-61
3. Lateral Weir Coefficient ±25%	6.96836E-15	1.96	3.555E-15	1	3.555E-15	691	2.31217E-61
4. Drag Coefficient of Bridges ±25%	2.64776E-13	1.96	1.351E-13	1	1.351E-13	777	4.28619E-55
5. Bridge Weir Coefficient ±25%	2.99612E-13	1.96	1.529E-13	1	1.529E-13	791	6.90296E-55
				$\Sigma u_i^2=$	0.0304885	Σ=	1.06599E-06
				$u_c=$	0.1746095		
				$u_c^4=$	0.0009295	$v_{eff}=$	872
						k=	1.9629
			Max WSE=	28.7 m	*U* @.95% Conf. Lev. =		**±0.3427**

Table A 2: Calculation table of XS 1765 on Çam Creek Upstream

R1R1_1765	Component Values						
Uncertainty Components	U_i	k_i	$u(x_i)$	c_i	$\|c_i.u(x_i)\|$	v_i	$\|c_i.u(x_i)\|^4/v_i$
1. Manning n coefficient ±25%	0.308168574	1.96	0.1572289	1	0.1572289	872	7.0083E-07
2. Downstream Boundry Condition ±15%	9.50383E-05	1.96	4.849E-05	1	4.849E-05	692	7.98847E-21
3. Lateral Weir Coefficient ±25%	7.87424E-13	1.96	4.017E-13	1	4.017E-13	691	3.76992E-53
4. Drag Coefficient of Bridges ±25%	8.77943E-13	1.96	4.479E-13	1	4.479E-13	777	5.18107E-53
5. Bridge Weir Coefficient ±25%	8.91868E-13	1.96	4.55E-13	1	4.55E-13	791	5.42003E-53
				$\Sigma u_i^2=$	0.0247209	Σ=	7.0083E-07
				$u_c=$	0.1572289		
				$u_c^4=$	0.0006111	$v_{eff}=$	872.0001659
						k=	1.9629
			Max WSE=	25.43 m	*U* @.95% Conf. Lev. =		**±0.3086**

Table A 3: Calculation table of XS 1569 on Çam Creek Upstream

R1R1_1569	Component Values						
Uncertainty Components	U_i	k_i	$u(x_i)$	c_i	$\|c_i.u(x_i)\|$	v_i	$\|c_i.u(x_i)\|^4/v_i$
1. Manning n coefficient ±25%	0.339981939	1.96	0.1734602	1	0.1734602	872	1.0382E-06
2. Downstream Boundry Condition ±15%	0.000138041	1.96	7.043E-05	1	7.043E-05	692	3.55551E-20
3. Lateral Weir Coefficient ±25%	8.14815E-05	1.96	4.157E-05	1	4.157E-05	691	4.32249E-21
4. Drag Coefficient of Bridges ±25%	9.22226E-05	1.96	4.705E-05	1	4.705E-05	777	6.30818E-21
5. Bridge Weir Coefficient ±25%	0.000809174	1.96	0.0004128	1	0.0004128	791	3.67255E-17
				$\Sigma u_i^2=$	0.0300886	Σ=	1.0382E-06
				$u_c=$	0.1734607		
				$u_c^4=$	0.0009053	$v_{eff}=$	872.0103951
						k=	1.9629
			Max WSE=	23.5 m	*U* @.95% Conf. Lev. =		**±0.3405**

Table A 4: Calculation table of XS 1429 on Çam Creek Upstream

R1R1_1429	Component Values						
Uncertainty Components	U_i	k_i	$u(x_i)$	c_i	$\|c_i.u(x_i)\|$	v_i	$\|c_i.u(x_i)\|^4/v_i$
1. Manning n coefficient ±25%	0.155447476	1.96	0.0793099	1	0.0793099	872	4.53726E-08
2. Downstream Boundry Condition ±15%	0.039686864	1.96	0.0202484	1	0.0202484	692	2.42916E-10
3. Lateral Weir Coefficient ±25%	0.012419158	1.96	0.0063363	1	0.0063363	691	2.33274E-12
4. Drag Coefficient of Bridges ±25%	0.010918536	1.96	0.0055707	1	0.0055707	777	1.2394E-12
5. Bridge Weir Coefficient ±25%	0.010284568	1.96	0.0052472	1	0.0052472	791	9.58393E-13
				Σu_i^2=	0.0067988	Σ=	4.56201E-08
				u_c=	0.0824547		
				u_c^4=	4.622E-05	v_{eff}=	1013.224746
						k=	1.9625
			Max WSE=	21.88 m	*U* @.95% Conf. Lev. =		**±0.1618**

Table A 5: Calculation table of XS 1324 on Çam Creek Downstream

R1R1Low_1324	Component Values						
Uncertainty Components	U_i	k_i	$u(x_i)$	c_i	$\|c_i.u(x_i)\|$	v_i	$\|c_i.u(x_i)\|^4/v_i$
1. Manning n coefficient ±25%	0.318809704	1.96	0.162658	1	0.162658	872	8.02759E-07
2. Downstream Boundry Condition ±15%	0.00167517	1.96	0.0008547	1	0.0008547	692	7.7109E-16
3. Lateral Weir Coefficient ±25%	0.001871305	1.96	0.0009547	1	0.0009547	691	1.20248E-15
4. Drag Coefficient of Bridges ±25%	0.000312849	1.96	0.0001596	1	0.0001596	777	8.35395E-19
5. Bridge Weir Coefficient ±25%	0.007470989	1.96	0.0038117	1	0.0038117	791	2.66877E-13
				Σu_i^2=	0.0264738	Σ=	8.0276E-07
				u_c=	0.1627078		
				u_c^4=	0.0007009	v_{eff}=	873.0676726
						k=	1.9629
			Max WSE=	20.7 m	*U* @.95% Conf. Lev. =		**±0.3194**

Table A 6: Calculation table of XS 1160 on Çam Creek Downstream

R1R1Low_1160	Component Values						
Uncertainty Components	U_i	k_i	$u(x_i)$	c_i	$\|c_i.u(x_i)\|$	v_i	$\|c_i.u(x_i)\|^4/v_i$
1. Manning n coefficient ±25%	0.261657501	1.96	0.1334987	1	0.1334987	872	3.64244E-07
2. Downstream Boundry Condition ±15%	0.000384717	1.96	0.0001963	1	0.0001963	692	2.14503E-18
3. Lateral Weir Coefficient ±25%	0.000915884	1.96	0.0004673	1	0.0004673	691	6.90015E-17
4. Drag Coefficient of Bridges ±25%	0.000171952	1.96	8.773E-05	1	8.773E-05	777	7.62402E-20
5. Bridge Weir Coefficient ±25%	0.000774384	1.96	0.0003951	1	0.0003951	791	3.08053E-17
				Σu_i^2=	0.0178223	Σ=	3.64244E-07
				u_c=	0.1335003		
				u_c^4=	0.0003176	v_{eff}=	872.0411669
						k=	1.9629
			Max WSE=	18.51 m	*U* @.95% Conf. Lev. =		**±0.2620**

Table A 7: Calculation table of XS 580 on Çam Creek Downstream

R1R1Low_580	Component Values						
Uncertainty Components	U_i	k_i	$u(x_i)$	c_i	$\lvert c_i.u(x_i)\rvert$	v_i	$\lvert c_i.u(x_i)\rvert^4/v_i$
1. Manning n coefficient ±25%	0.229337132	1.96	0.1170087	1	0.1170087	872	2.1496E-07
2. Downstream Boundry Condition ±15%	0.000593957	1.96	0.000303	1	0.000303	692	1.21868E-17
3. Lateral Weir Coefficient ±25%	0.00069236	1.96	0.0003532	1	0.0003532	691	2.25334E-17
4. Drag Coefficient of Bridges ±25%	0.000113644	1.96	5.798E-05	1	5.798E-05	777	1.45457E-20
5. Bridge Weir Coefficient ±25%	0.000570908	1.96	0.0002913	1	0.0002913	791	9.10045E-18
				Σu_i^2=	0.0136914	Σ=	2.1496E-07
				u_c=	0.11701		
				u_c^4=	0.0001875	v_{eff}=	872.0388291
						k=	1.9629
			Max WSE=	9.875 m	*U* @.95% Conf. Lev. =		**±0.2297**

Table A 8: Calculation table of XS 340 on Çam Creek Downstream

R1R1Low_340	Component Values						
Uncertainty Components	U_i	k_i	$u(x_i)$	c_i	$\lvert c_i.u(x_i)\rvert$	v_i	$\lvert c_i.u(x_i)\rvert^4/v_i$
1. Manning n coefficient ±25%	0.325310134	1.96	0.1659746	1	0.1659746	872	8.70261E-07
2. Downstream Boundry Condition ±15%	0.001540874	1.96	0.0007862	1	0.0007862	692	5.51998E-16
3. Lateral Weir Coefficient ±25%	0.002772107	1.96	0.0014143	1	0.0014143	691	5.79078E-15
4. Drag Coefficient of Bridges ±25%	0.000373533	1.96	0.0001906	1	0.0001906	777	1.69774E-18
5. Bridge Weir Coefficient ±25%	0.002710242	1.96	0.0013828	1	0.0013828	791	4.62202E-15
				Σu_i^2=	0.0275521	Σ=	8.70261E-07
				u_c=	0.1659883		
				u_c^4=	0.0007591	v_{eff}=	872.289131
						k=	1.9629
			Max WSE=	7.107 m	*U* @.95% Conf. Lev. =		**±0.3258**

Table A 9: Calculation table of XS 140 on Çam Creek Downstream

R1R1Low_140	Component Values						
Uncertainty Components	U_i	k_i	$u(x_i)$	c_i	$\lvert c_i.u(x_i)\rvert$	v_i	$\lvert c_i.u(x_i)\rvert^4/v_i$
1. Manning n coefficient ±25%	0.453509744	1.96	0.2313825	1	0.2313825	872	3.28705E-06
2. Downstream Boundry Condition ±15%	0.006071583	1.96	0.0030977	1	0.0030977	692	1.33069E-13
3. Lateral Weir Coefficient ±25%	0.0050799	1.96	0.0025918	1	0.0025918	691	6.53008E-14
4. Drag Coefficient of Bridges ±25%	0.00325054	1.96	0.0016584	1	0.0016584	777	9.73591E-15
5. Bridge Weir Coefficient ±25%	0.008024394	1.96	0.0040941	1	0.0040941	791	3.5518E-13
				Σu_i^2=	0.0535737	Σ=	3.28705E-06
				u_c=	0.2314599		
				u_c^4=	0.0028701	v_{eff}=	873.167252
						k=	1.9629
			Max WSE=	5.161 m	*U* @.95% Conf. Lev. =		**±0.4543**

Table A 10: Calculation table of XS 72 on Çam Creek Downstream

R1R1Low_72	Component Values						
Uncertainty Components	U_i	k_i	$u(x_i)$	c_i	$\lvert c_i.u(x_i)\rvert$	v_i	$\lvert c_i.u(x_i)\rvert^4/v_i$
1. Manning n coefficient ±25%	0.3013313	1.96	0.1537405	1	0.1537405	872	6.40673E-07
2. Downstream Boundry Condition ±15%	0.007143363	1.96	0.0036446	1	0.0036446	692	2.54965E-13
3. Lateral Weir Coefficient ±25%	0.002283145	1.96	0.0011649	1	0.0011649	691	2.6646E-15
4. Drag Coefficient of Bridges ±25%	0.007081113	1.96	0.0036128	1	0.0036128	777	2.19261E-13
5. Bridge Weir Coefficient ±25%	0.012002687	1.96	0.0061238	1	0.0061238	791	1.77792E-12
				Σu_i^2=	0.0237013	Σ=	6.40675E-07
				u_c=	0.1539523		
				u_c^4=	0.0005618	v_{eff}=	876.813867
						k=	1.9629
			Max WSE=	4.545 m	*U* @.95% Conf. Lev. =		**±0.3022**

Table A 11: Calculation table of XS 4 on Çam Creek Downstream

R1R1Low_4	Component Values						
Uncertainty Components	U_i	k_i	$u(x_i)$	c_i	$\lvert c_i.u(x_i)\rvert$	v_i	$\lvert c_i.u(x_i)\rvert^4/v_i$
1. Manning n coefficient ±25%	0.342857346	1.96	0.1749272	1	0.1749272	872	1.07377E-06
2. Downstream Boundry Condition ±15%	0.105843423	1.96	0.0540017	1	0.0540017	692	1.22892E-08
3. Lateral Weir Coefficient ±25%	0.00312697	1.96	0.0015954	1	0.0015954	691	9.37546E-15
4. Drag Coefficient of Bridges ±25%	0.001094993	1.96	0.0005587	1	0.0005587	777	1.25372E-16
5. Bridge Weir Coefficient ±25%	0.008385239	1.96	0.0042782	1	0.0042782	791	4.23507E-13
				Σu_i^2=	0.0335369	Σ=	1.08606E-06
				u_c=	0.1831308		
				u_c^4=	0.0011247	v_{eff}=	1035.594777
						k=	1.9624
			Max WSE=	3.034 m	*U* @.95% Conf. Lev. =		**±0.3594**

Table A 12: Calculation table of XS 696 on Köprücü Creek

R2R1_696	Component Values						
Uncertainty Components	U_i	k_i	$u(x_i)$	c_i	$\lvert c_i.u(x_i)\rvert$	v_i	$\lvert c_i.u(x_i)\rvert^4/v_i$
1. Manning n coefficient ±25%	0.283227947	1.96	0.1445041	1	0.1445041	872	5.00039E-07
2. Downstream Boundry Condition ±15%	2.50861E-13	1.96	1.28E-13	1	1.28E-13	692	3.87792E-55
3. Lateral Weir Coefficient ±25%	0.000409221	1.96	0.0002088	1	0.0002088	691	2.74999E-18
4. Drag Coefficient of Bridges ±25%	1.10091E-12	1.96	5.617E-13	1	5.617E-13	777	1.28105E-52
5. Bridge Weir Coefficient ±25%	0.000152785	1.96	7.795E-05	1	7.795E-05	791	4.66791E-20
				Σu_i^2=	0.0208815	Σ=	5.00039E-07
				u_c=	0.1445042		
				u_c^4=	0.000436	v_{eff}=	872.0041482
						k=	1.9629
			Max WSE=	37.63 m	*U* @.95% Conf. Lev. =		**±0.2836**

Table A 13: Calculation table of XS 500 on Köprücü Creek

R2R1_500	Component Values						
Uncertainty Components	U_i	k_i	$u(x_i)$	c_i	$\|c_i.u(x_i)\|$	v_i	$\|c_i.u(x_i)\|^4/v_i$
1. Manning n coefficient ±25%	0.052568053	1.96	0.0268204	1	0.0268204	872	5.93399E-10
2. Downstream Boundry Condition ±15%	3.20544E-13	1.96	1.635E-13	1	1.635E-13	692	1.03376E-54
3. Lateral Weir Coefficient ±25%	0.028672155	1.96	0.0146287	1	0.0146287	691	6.62734E-11
4. Drag Coefficient of Bridges ±25%	5.99231E-13	1.96	3.057E-13	1	3.057E-13	777	1.12443E-53
5. Bridge Weir Coefficient ±25%	0.069596769	1.96	0.0355086	1	0.0355086	791	2.00981E-09
				Σu_i^2=	0.0021942	Σ=	2.66948E-09
				u_c=	0.0468422		
				u_c^4=	4.814E-06	v_{eff}=	1803.521273
						k=	1.9614
			Max WSE=	34.55 m	*U* @.95% Conf. Lev. =		**±0.0919**

Table A 14: Calculation table of XS 404 on Köprücü Creek

R2R1_404	Component Values						
Uncertainty Components	U_i	k_i	$u(x_i)$	c_i	$\|c_i.u(x_i)\|$	v_i	$\|c_i.u(x_i)\|^4/v_i$
1. Manning n coefficient ±25%	0.240310785	1.96	0.1226075	1	0.1226075	872	2.59151E-07
2. Downstream Boundry Condition ±15%	4.94753E-13	1.96	2.524E-13	1	2.524E-13	692	5.86709E-54
3. Lateral Weir Coefficient ±25%	0.001155564	1.96	0.0005896	1	0.0005896	691	1.74853E-16
4. Drag Coefficient of Bridges ±25%	3.27487E-13	1.96	1.671E-13	1	1.671E-13	777	1.00306E-54
5. Bridge Weir Coefficient ±25%	0.020312742	1.96	0.0103636	1	0.0103636	791	1.45839E-11
				Σu_i^2=	0.0151404	Σ=	2.59165E-07
				u_c=	0.1230462		
				u_c^4=	0.0002292	v_{eff}=	884.4958985
						k=	1.9628
			Max WSE=	30.45 m	*U* @.95% Conf. Lev. =		**±0.2415**

Table A 15: Calculation table of XS 132 on Köprücü Creek

R2R1_132	Component Values						
Uncertainty Components	U_i	k_i	$u(x_i)$	c_i	$\|c_i.u(x_i)\|$	v_i	$\|c_i.u(x_i)\|^4/v_i$
1. Manning n coefficient ±25%	0.232989414	1.96	0.1188722	1	0.1188722	872	2.28983E-07
2. Downstream Boundry Condition ±15%	0.000232509	1.96	0.0001186	1	0.0001186	692	2.86175E-19
3. Lateral Weir Coefficient ±25%	0.001183441	1.96	0.0006038	1	0.0006038	691	1.92346E-16
4. Drag Coefficient of Bridges ±25%	0.000210417	1.96	0.0001074	1	0.0001074	777	1.70954E-19
5. Bridge Weir Coefficient ±25%	0.018494437	1.96	0.0094359	1	0.0094359	791	1.00222E-11
				Σu_i^2=	0.01422	Σ=	2.28993E-07
				u_c=	0.1192477		
				u_c^4=	0.0002022	v_{eff}=	883.0333831
						k=	1.9628
			Max WSE=	23.39 m	*U* @.95% Conf. Lev. =		**±0.2341**

Table A 16: Calculation table of XS 44 on Köprücü Creek

R2R1_44	Component Values						
Uncertainty Components	U_i	k_i	$u(x_i)$	c_i	$\lvert c_i.u(x_i)\rvert$	v_i	$\lvert c_i.u(x_i)\rvert^4/v_i$
1. Manning n coefficient ±25%	0.126629578	1.96	0.0646069	1	0.0646069	872	1.99802E-08
2. Downstream Boundry Condition ±15%	0.045280094	1.96	0.0231021	1	0.0231021	692	4.11622E-10
3. Lateral Weir Coefficient ±25%	0.012313191	1.96	0.0062822	1	0.0062822	691	2.25414E-12
4. Drag Coefficient of Bridges ±25%	0.014045347	1.96	0.007166	1	0.007166	777	3.39379E-12
5. Bridge Weir Coefficient ±25%	0.018983541	1.96	0.0096855	1	0.0096855	791	1.11252E-11
				$\Sigma u_i^2=$	0.0048924	$\Sigma=$	2.04086E-08
				$u_c=$	0.0699456		
				$u_c^4=$	2.394E-05	$v_{eff}=$	1172.812688
						k=	1.9621
			Max WSE=	22.02 m	*U* @.95% Conf. Lev. =		**±0.1372**

B. Uncertainty Budget Tables of Selected 2D Computational Cells

Uncertainty Budget Tables of 2D cells in Perimeter-1 (Annotation: Perimeter No_ Cell Name):

Table B 1: Calculation table of 2D Cells No:7 on Perimeter 1

P1_7	Component Values						
Uncertainty Components	U_i	k_i	$u(x_i)$	c_i	$\lvert c_i.u(x_i)\rvert$	v_i	$\lvert c_i.u(x_i)\rvert^4/v_i$
1. Manning n coefficient ±25%	0.51560415	1.96	0.26306334	1	0.2630633	870	5.50455E-06
2. Downstream Boundry Condition ±15%	4.87784E-13	1.96	2.4887E-13	1	2.489E-13	692	5.54346E-54
3. Lateral Weir Coefficient ±25%	0.039581206	1.96	0.02019449	1	0.0201945	592	2.80938E-10
				$\Sigma u_i^2=$	0.0696101	$\Sigma=$	5.50483E-06
				$u_c=$	0.2638373		
				$u_c^4=$	0.0048456	$v_{eff}=$	880.2393167
						k=	1.9628
			Max WSE=	23.5 m	U @.95% Conf. Lev. =		**±0.5179**

Table B 2: Calculation table of 2D Cells No:78 on Perimeter 1

P1_78	Component Values						
Uncertainty Components	U_i	k_i	$u(x_i)$	c_i	$\lvert c_i.u(x_i)\rvert$	v_i	$\lvert c_i.u(x_i)\rvert^4/v_i$
1. Manning n coefficient ±25%	0.480055263	1.96	0.24492615	1	0.2449262	870	4.13639E-06
2. Downstream Boundry Condition ±15%	4.87784E-13	1.96	2.4887E-13	1	2.489E-13	692	5.54346E-54
3. Lateral Weir Coefficient ±25%	0.039580261	1.96	0.02019401	1	0.020194	592	2.80911E-10
				$\Sigma u_i^2=$	0.0603966	$\Sigma=$	4.13667E-06
				$u_c=$	0.2457572		
				$u_c^4=$	0.0036478	$v_{eff}=$	881.808666
						k=	1.9628
			Max WSE=	23.5 m	U @.95% Conf. Lev. =		**±0.4824**

Table B 3: Calculation table of 2D Cells No:109 on Perimeter 1

P1_109	Component Values						
Uncertainty Components	U_i	k_i	$u(x_i)$	c_i	$\lvert c_i.u(x_i)\rvert$	v_i	$\lvert c_i.u(x_i)\rvert^4/v_i$
1. Manning n coefficient ±25%	0.379092856	1.96	0.19341472	1	0.1934147	870	1.60857E-06
2. Downstream Boundry Condition ±15%	8.45609E-05	1.96	4.3143E-05	1	4.314E-05	692	5.00666E-21
3. Lateral Weir Coefficient ±25%	0.003951019	1.96	0.00201583	1	0.0020158	592	2.78927E-14
				$\Sigma u_i^2=$	0.0374133	$\Sigma=$	1.60857E-06
				$u_c=$	0.1934252		
				$u_c^4=$	0.0013998	$v_{eff}=$	870.1890881
						k=	1.9629
			Max WSE=	23.5 m	U @.95% Conf. Lev. =		**±0.3797**

Table B 4: Calculation table of 2D Cells No:1158 on Perimeter 1

P1_1158	Component Values						
Uncertainty Components	U_i	k_i	$u(x_i)$	c_i	$\|c_i.u(x_i)\|$	v_i	$\|c_i.u(x_i)\|^4/v_i$
1. Manning n coefficient ±25%	0.501572805	1.96	0.25590449	1	0.2559045	870	4.92938E-06
2. Downstream Boundry Condition ±15%	4.87784E-13	1.96	2.4887E-13	1	2.489E-13	692	5.54346E-54
3. Lateral Weir Coefficient ±25%	0.039581206	1.96	0.02019449	1	0.0201945	592	2.80938E-10
				Σu_i^2=	0.0658949	Σ=	4.92966E-06
				u_c=	0.2567001		
				u_c^4=	0.0043421	v_{eff}=	880.8192983
						k=	1.9628
			Max WSE=	23.5 m	*U* @.95% Conf. Lev. =		**±0.5039**

Table B 5: Calculation table of 2D Cells No:30 on Perimeter 2

P2_30	Component Values						
Uncertainty Components	U_i	k_i	$u(x_i)$	c_i	$\|c_i.u(x_i)\|$	v_i	$\|c_i.u(x_i)\|^4/v_i$
1. Manning n coefficient ±25%	0.391178754	1.96	0.199581	1	0.199581	870	1.82372E-06
2. Downstream Boundry Condition ±15%	0.000232681	1.96	0.00011871	1	0.0001187	692	2.87021E-19
3. Lateral Weir Coefficient ±25%	0.010350612	1.96	0.00528092	1	0.0052809	592	1.31377E-12
				Σu_i^2=	0.0398605	Σ=	1.82372E-06
				u_c=	0.1996509		
				u_c^4=	0.0015889	v_{eff}=	871.218649
						k=	1.9629
			Max WSE=	11.82 m	*U* @.95% Conf. Lev. =		**±0.3919**

Table B 6: Calculation table of 2D Cells No:85 on Perimeter 2

P2_85	Component Values						
Uncertainty Components	U_i	k_i	$u(x_i)$	c_i	$\|c_i.u(x_i)\|$	v_i	$\|c_i.u(x_i)\|^4/v_i$
1. Manning n coefficient ±25%	0.276942329	1.96	0.14129711	1	0.1412971	870	4.58156E-07
2. Downstream Boundry Condition ±15%	0.000896691	1.96	0.0004575	1	0.0004575	692	6.33054E-17
3. Lateral Weir Coefficient ±25%	0.001772632	1.96	0.0009044	1	0.0009044	592	1.13013E-15
				Σu_i^2=	0.0199659	Σ=	4.58156E-07
				u_c=	0.1413007		
				u_c^4=	0.0003986	v_{eff}=	870.0895279
						k=	1.9629
			Max WSE=	9.576 m	*U* @.95% Conf. Lev. =		**±0.2774**

Table B 7: Calculation table of 2D Cells No:461 on Perimeter 2

P2_461	Component Values						
Uncertainty Components	U_i	k_i	$u(x_i)$	c_i	$\|c_i.u(x_i)\|$	v_i	$\|c_i.u(x_i)\|^4/v_i$
1. Manning n coefficient ±25%	0.068259221	1.96	0.03482613	1	0.0348261	870	1.69084E-09
2. Downstream Boundry Condition ±15%	0.000624383	1.96	0.00031856	1	0.0003186	692	1.48824E-17
3. Lateral Weir Coefficient ±25%	0.003328076	1.96	0.001698	1	0.001698	592	1.40419E-14
				Σu_i^2=	0.0012158	Σ=	1.69085E-09
				u_c=	0.034869		
				u_c^4=	1.478E-06	v_{eff}=	874.2798981
						k=	1.9629
			Max WSE=	7.734 m	*U* @.95% Conf. Lev. =		**±0.0684**

Table B 8: Calculation table of 2D Cells No:2705 on Perimeter 2

P2_2705	Component Values						
Uncertainty Components	U_i	k_i	$u(x_i)$	c_i	$\lvert c_i.u(x_i)\rvert$	v_i	$\lvert c_i.u(x_i)\rvert^4/v_i$
1. Manning n coefficient ±25%	0.430882639	1.96	0.21983808	1	0.2198381	870	2.68468E-06
2. Downstream Boundry Condition ±15%	0.000247334	1.96	0.00012619	1	0.0001262	692	3.66441E-19
3. Lateral Weir Coefficient ±25%	0.006743602	1.96	0.00344061	1	0.0034406	592	2.36713E-13
				Σu_i^2=	0.0483406	Σ=	2.68468E-06
				u_c=	0.219865		
				u_c^4=	0.0023368	v_{eff}=	870.4267505
						k=	1.9629
			Max WSE=	11.51 m	*U* @.95% Conf. Lev. =		**±0.4316**

Table B 9: Calculation table of 2D Cells No:2766 on Perimeter 2

P2_2766	Component Values						
Uncertainty Components	U_i	k_i	$u(x_i)$	c_i	$\lvert c_i.u(x_i)\rvert$	v_i	$\lvert c_i.u(x_i)\rvert^4/v_i$
1. Manning n coefficient ±25%	0.061543419	1.96	0.0313997	1	0.0313997	870	1.11733E-09
2. Downstream Boundry Condition ±15%	0.00067972	1.96	0.0003468	1	0.0003468	692	2.09021E-17
3. Lateral Weir Coefficient ±25%	0.002964949	1.96	0.00151273	1	0.0015127	592	8.84551E-15
				Σu_i^2=	0.0009884	Σ=	1.11734E-09
				u_c=	0.031438		
				u_c^4=	9.768E-07	v_{eff}=	874.2490062
						k=	1.9629
			Max WSE=	5.981 m	*U* @.95% Conf. Lev. =		**±0.0617**

Uncertainty Budget Tables of 2D cells in Perimeter-3 (Annotation: Perimeter No_ Cell Name):

Table B 10: Calculation table of 2D Cells No:428 on Perimeter 3

P3_428	Component Values						
Uncertainty Components	U_i	k_i	$u(x_i)$	c_i	$\lvert c_i.u(x_i)\rvert$	v_i	$\lvert c_i.u(x_i)\rvert^4/v_i$
1. Manning n coefficient ±25%	4.56357E-13	1.96	2.3284E-13	1	2.328E-13	870	3.37812E-54
2. Downstream Boundry Condition ±15%	1.21946E-13	1.96	6.2217E-14	1	6.222E-14	692	2.16542E-56
3. Lateral Weir Coefficient ±25%	6.9692E-14	1.96	3.5557E-14	1	3.556E-14	592	2.70013E-57
				Σu_i^2=	5.935E-26	Σ=	3.40248E-54
				u_c=	2.436E-13		
				u_c^4=	3.522E-51	v_{eff}=	1035.166988
						k=	1.9624
			Max WSE=	13.27 m	*U* @.95% Conf. Lev. =		**±0.0000**

Table B 11: Calculation table of 2D Cells No:712 on Perimeter 3

P3_712	Component Values						
Uncertainty Components	U_i	k_i	$u(x_i)$	c_i	$\|c_i.u(x_i)\|$	v_i	$\|c_i.u(x_i)\|^4/v_i$
1. Manning n coefficient ±25%	0.39354537	1.96	0.20078845	1	0.2007885	870	1.86825E-06
2. Downstream Boundry Condition ±15%	0.000284515	1.96	0.00014516	1	0.0001452	692	6.4164E-19
3. Lateral Weir Coefficient ±25%	0.017881136	1.96	0.00912303	1	0.009123	592	1.17013E-11
				Σu_i^2=	0.0403993	Σ=	1.86826E-06
				u_c=	0.2009957		
				u_c^4=	0.0016321	v_{eff}=	873.5912593
						k=	1.9629
			Max WSE=	10.49 m	*U* @.95% Conf. Lev. =		**±0.3945**

Table B 12: Calculation table of 2D Cells No:1013 on Perimeter 3

P3_1013	Component Values						
Uncertainty Components	U_i	k_i	$u(x_i)$	c_i	$\|c_i.u(x_i)\|$	v_i	$\|c_i.u(x_i)\|^4/v_i$
1. Manning n coefficient ±25%	0.303823935	1.96	0.15501221	1	0.1550122	870	6.63658E-07
2. Downstream Boundry Condition ±15%	0.003712749	1.96	0.00189426	1	0.0018943	692	1.86059E-14
3. Lateral Weir Coefficient ±25%	0.004546504	1.96	0.00231965	1	0.0023196	592	4.89063E-14
				Σu_i^2=	0.0240378	Σ=	6.63658E-07
				u_c=	0.1550411		
				u_c^4=	0.0005778	v_{eff}=	870.6495041
						k=	1.9629
			Max WSE=	8.851 m	*U* @.95% Conf. Lev. =		**±0.3043**

Table B 13: Calculation table of 2D Cells No:1456 on Perimeter 3

P3_1456	Component Values						
Uncertainty Components	U_i	k_i	$u(x_i)$	c_i	$\|c_i.u(x_i)\|$	v_i	$\|c_i.u(x_i)\|^4/v_i$
1. Manning n coefficient ±25%	0.663134642	1.96	0.338334	1	0.338334	870	1.50613E-05
2. Downstream Boundry Condition ±15%	2.94572E-05	1.96	1.5029E-05	1	1.503E-05	692	7.3728E-23
3. Lateral Weir Coefficient ±25%	0.000633599	1.96	0.00032326	1	0.0003233	592	1.84464E-17
				Σu_i^2=	0.11447	Σ=	1.50613E-05
				u_c=	0.3383342		
				u_c^4=	0.0131034	v_{eff}=	870.0015919
						k=	1.9629
			Max WSE=	14.54 m	*U* @.95% Conf. Lev. =		**±0.6641**

Table B 14: Calculation table of 2D Cells No:1751 on Perimeter 3

P3_1751	Component Values						
Uncertainty Components	U_i	k_i	$u(x_i)$	c_i	$\|c_i.u(x_i)\|$	v_i	$\|c_i.u(x_i)\|^4/v_i$
1. Manning n coefficient ±25%	0.204164263	1.96	0.10416544	1	0.1041654	870	1.35324E-07
2. Downstream Boundry Condition ±15%	6.14852E-05	1.96	3.137E-05	1	3.137E-05	692	1.39943E-21
3. Lateral Weir Coefficient ±25%	0.000141526	1.96	7.2207E-05	1	7.221E-05	592	4.59196E-20
				Σu_i^2=	0.0108504	Σ=	1.35324E-07
				u_c=	0.1041655		
				u_c^4=	0.0001177	v_{eff}=	870.0009939
						k=	1.9629
			Max WSE=	16.42 m	*U* @.95% Conf. Lev. =		**±0.2045**